Basin Research

IAS EAGE

The Svalbard Eocene-Oligocene (?) Central Basin succession: Sedimentation patterns and controls

Journal:	*Basin Research*
Manuscript ID	BRE-086-2020
Manuscript Type:	Original Article
Date Submitted by the Author:	16-Apr-2020
Complete List of Authors:	Helland-Hansen, William; Universitetet i Bergen Det Matematisk-naturvitenskapelige Fakultet, Department of Earth Science; Grundvåg, Sten-Andreas; UiT The Arctic University of Norway, Department of Geosciences
Keywords:	foreland basins, tectonics and sedimentation, sedimentology, Svalbard, basin filling

The Svalbard Eocene-Oligocene (?) Central Basin succession: Sedimentation patterns and controls

William Helland-Hansen[1,2] and Sten-Andreas Grundvåg[3]

[1]Department of Earth Science, University of Bergen

[2]UNIS, Svalbard

[3] Department of Geosciences, UiT - The Arctic University of Norway

ACKNOWLEDGMENTS

Thanks to Tore Aadland and Atle Rotevatn who gave constructive feedback to parts of earlier versions of this manuscript. Eva Bjørseth drafted figures 8, 9 and 10. Sten-Andreas Grundvåg received funding from the ARCEx project (Research Centre for Arctic Petroleum Exploration), which is funded by the Research Council of Norway (grant number 228107).

DATA AVAILABILITY STATEMENT

The data that support the findings of this study are available from the corresponding author upon reasonable request.

ABSTRACT

A synthesis has been undertaken based on regionally compiled data from the post early Eocene foreland basin succession of Svalbard. The aim has been to generate an updated depositional model and link this to controlling factors. The more than kilometer thick progradational succession includes the offshore shales of the Gilsonryggen Member, the shallow marine sandstones of the Battfjellet Formation and the predominantly heterolithic Aspelintoppen Formation, together recording the progressive eastwards infill of the foredeep flanking the West Spitsbergen fold-and-thrust belt.

Here we present a summary of the environmental elements across the basin, their facies and regional distribution and link these together in an updated depositional model. The system prograded with an ascending trajectory in the order of 1°. The basin fill was bipartite, with

offset stacked shelf and shelf-edge deltas, slope clinothems and basin floor fans in the western and deepest part and a simpler architecture of stacked shelf-deltas in the shallower eastern part. A comprehensive discussion on basin type, basin forming processes, the role of subsidence, eustasy and sediment supply as well as the beyond-outcrop extent of the system is given. We suggest a foredeep setting governed by flexural loading, likely influenced by buckling, and potentially developing into a wedge top basin in the mature stage of basin filling. High-subsidence rates probably counteracted eustatic falls with the result that relative sea-level falls concomitant with deposition were uncommon. Distance to the source terrain was small and sedimentation rates was temporarily high. Time-equivalent deposits can be found outbound of Stappen High in the Vestbakken Volcanic Province and the Sørvestsnaget Basin further south on the Barents Shelf margin. We cannot see any direct evidence of coupling between these more southerly systems and the studied one; southerly diversion of the sediment-routing, if any, may have taken place beyond the limit of the preserved deposits.

KEYWORDS: Svalbard, Spitsbergen, foreland basin, Paleogene, Eocene, Central Basin

INTRODUCTION

Rationale and aims

The main sedimentary response to the Paleogene uplift of the West Spitsbergen Fold-and-Thrust Belt (WSFTB) (Figure 1), the kilometer-scale thick progradational succession containing the Gilsonryggen Member of the Frysjaodden Formation (offshore), the Battfjellet Formation (shallow marine) and the Aspelintoppen Formation (continental) (Nathorst, 1910; Atkinson, 1963; Major & Nagy, 1972; Kellogg, 1975; Steel, 1977; Steel et al., 1981; Steel et al., 1985; Helland-Hansen, 1990; Dallmann, 1999) (Figure 2 and 3) has long been used as a scientific and educational laboratory. The extraordinary good exposures of both kilometer-scale geometries as well as close-up facies-scale excellently demonstrates aspects related to foreland basin sedimentation, the spatial-temporal illustration of continental to submarine systems tracts, the coupling of seismic scale geometries to outcrops and subsurface, the process understanding of clinoform deposition and the link between coastal sedimentation and basin floor mass-gravity deposition. More than 10 MSc theses and 30 publications have emanated from studies of this succession over the last 15 years and more than thousand students and numerous oil-company field excursions have visited the succession to gain knowledge about the abovementioned factors and relate them to subsurface systems.

Based on our own unpublished and published work and theses of MSc students we have supervised (see section *Data* below) we give an updated and comprehensive overview of the paleogeographic and tectonostratigraphic development of the succession. Specifically, we will focus on models for development and distribution of the main environmental elements of the system and how these are

connected, and discuss how these relate to the overall basin filling and which controls were instrumental in determining the character of basin filling. Specifically, a comprehensive review of the basin type and extent, and the impact of subsidence, eustasy and sediment supply on the basin-fill history will be presented, adding to the more fragmented contributions on these aspects in the literature for this part of the Svalbard stratigraphy.

Geological setting

The regressive megasequence of the combined Gilsonryggen Member, Battfjellet Formation and Aspelintoppen Formation (hereafter referred to as the GBA-unit) constitutes the upper part of the Paleogene Van Mijenfjorden Group in the Central Basin of Svalbard (Figure 2 and 3) (Steel et.al., 1981, 1985; Helland-Hansen, 1990; Bruhn & Steel, 2003). The GBA-unit prograded from the West Spitsbergen Fold-and Thrust Belt (WSFTB) and eastwards into the flanking foreland basin from latest Paleocene and onwards and has a preserved thickness of more than 1500 m (Helland-Hansen, 1990). The west to east transport direction is evidenced by paleocurrent data across the basin as well as the direction of sloping and thinning of clinothems in the western part of the basin (Kellogg, 1975; Steel et., 1981, 1985; Helland-Hansen, 1990). The westerly derived clastic wedge of the upper Paleocene Hollendardalen Formation (Figure 2) below the GBA-unit indicates a drainage reversal relative to underlying formations of the Central Basin and is assumed to be an early record of uplift in the west, whereas the GBA-unit itself represents the main sedimentary response (Steel et al., 1981; Helland-Hansen, 1990).

The formation of the WSFTB was a response to the development of a sheared margin along the western Barents Shelf as a result of the opening of the North-Atlantic in early Paleogene. The 750 km of dextral movement that was accommodated between the Eurasian and Greenland plates (Gaina et al., 2009) gave a largely transtensive response at the southern part of the shear margin (the Senja Fracture Zone) (e.g. Faleide et al., 1993; Kristensen et al. 2018), whereas western Svalbard experienced 20–40 km of crustal shortening (Bergh et al., 1997) as a result of transpression along the Hornsund Fault Zone (Figure 1). The syncline of the present Central Basin and its stratigraphic fill is the uplifted and eroded remnants of the final foredeep of the WSFTB (Helland-Hansen, 1990; Dörr et al., 2013) that existed prior to break-up and opening of the sea-way between Greenland and Norway commencing in the earliest Oligocene (Chron 13, Faleide et al., 1993; Lundin & Doré, 2002).

Time constraints on both structuring and accompanying foreland basin deposition are relatively limited. Only a few datings within the basin fill has been published; one gives a Late Paleocene age based on dinoflagellate species within the lowermost part of the Frysjaodden Formation (below the Hollendardalen Formation, Figure 2) (cf. Manum & Throndsen, 1986, their Figure 6); another is dated to ca. 56 Ma at the level of the PETM (Paleocene-Eocene thermal maximum) close to the base of the GBA-unit using radiometric dating of bentonites in combination with astrochronology (Charles et al., 2011; Harding et al., 2011). Owing to the large thickness and the post late Paleocene age, most workers have assumed that the GBA-unit is dominantly of Eocene and possibly also of Oligocene age, however this is not substantiated by biostratigaphic data. An early Eocene age has been suggested for the Aspelintoppen Formation based on comparison with other Arctic floras (Manum & Throndsen, 1986; Kvacek, 1994; Golovneva, 2000).

Tegner et al. (2011) and Piepjohn et al. (2016) suggest that the WSFTB is equivalent to the Eurekan fold belts in North Greenland and Arctic Canada. Compression peaked at 47 – 49 Ma (mid Eocene) based on thermal resetting ages from Upper Cretaceous volcanic flows in North Greenland (Tegner et al., 2011). From 36 Ma and onwards the west Svalbard margin developed into a rifted margin (Eldholm et al., 1984; Faleide et al., 1993) and was subject to rift shoulder uplift with continued erosion (Dimakis et al., 1998; Dörr et al., 2013). In the late Neogene and Quaternary times, recurrent glaciations and erosion continued, with Svalbard currently being in the state of post-glacial isostatic uplift (e.g. Forman et al., 1995; Landvik et al., 1998; Knies et al., 2009).

Svalbard's paleolatitudal position was probably only a few degrees south of the present; Clifton (2012) suggests 75°N for the Central Basin during the deposition of the Aspelintoppen Formation. Temperatures were much warmer than today; Golovneva (2000) suggested a warm-temperate or moderately temperate climate with high precipitation rates in Svalbard in Paleogene times. Based on studies of plant material in the Aspelintoppen Formation, mean annual average temperatures were estimated to range from 9–17°C (Golovneva, 2000; Uhl et al., 2007; Clifton, 2012).

Several studies have recorded outsized clasts, also within the Gilsonryggen Member in the lower part of the GBA-unit, which may indicate rafting by temporal sea ice (Kellogg, 1975; Dalland, 1977) or transport by driftwood (Dalland, 1977; Birkenmajer & Narebski, 1963). Rafting by sea ice is in accordance with some of the paleofloristic studies that also infer freezing temperatures during winter months (Golovneva, 2000; Uhl et al., 2007). Furthermore, the basin had low salinity because of large freshwater input from advancing deltas in a setting of high precipitation rates and elevated terrestrial runoff (Uhl et al., 2007; Greenwood et al., 2010; Harding et al., 2011). In summary, the climatic proxies together indicate a general temperate warm climate, possibly with strong seasonal or temporal variations.

The basin fill

The preserved Central Basin foreland infill demonstrates a thinning of the marine part of the succession (the Hollendardalen Formation, the Gilsonryggen Member and the Battfjellet Formation) from the orogenic flank towards the basin, from more than 700 m in the west to 300 m in the eastern part (cf. Helland-Hansen, 1990). Present day erosion limits the thickness of this marine succession to be slightly above 700 m (Figure 4a) but it is reasonable to suggest that the succession had an initial thickness well above 800 m when extrapolating isopachs westwards into the deeply eroded areas (Figure 4b). The overlying continental strata (the Aspelintoppen Formation) define the present-day mountain tops in the basin; hence its original thickness is unclear. The maximum preserved thickness is inferred to be more than 1000 meters on the south side of Van Mijenfjorden (Steel et el., 1981). According to recent vitrinite-reflectance-based overburden models by Marshall et al. (2015), the maximum depth of burial of coal in the Firkanten Formation in the Colesdalen area (central part of Nordenskiöld Land in the Central Basin) was in the order of 2.3 km. These data in combination with thickness maps by Bruhn & Steel (2003) for the Paleogene formations indicates, in the position of the maximum preserved thickness of the Aspelintoppen Formation on the south side of Van Mijenfjorden, about 500 m of removed overburden.

The upper part of the marine basin fill (the upper Gilsonryggen Member and the Battfjellet Formation) shows a distinct bi-partitioning into a western and eastern basin-segment with

contrasting styles of basin fill (Helland-Hansen, 1990, 2010). Both sandstone clinothems 200–300 m high and basin-floor sandstones up to 60 m thick can clearly be seen along the mountainsides in the western part of the basin (Figure 5a). This is in contrast to the eastern part of the basin where no such features can be seen.

The sandstones of the Battfjellet and Aspelintoppen formations are generally poorly sorted lithic greywackes with a large fraction of rock fragments and organic matter (Nysæther, 1966; Helland-Hansen, 2010; Mansurbeg et al., 2012; Schlegel et al., 2013). The sand grain-size is typically not coarser than medium with very fine-grained sands constituting the volumetrically most important sand-fraction caliber (cf. Helland-Hansen, 2010; Grundvåg et al., 2014a, b). Occasionally, thin conglomeratic horizons may be present at the base of fluvial channels (Naurstad, 2014); however, this sediment caliber is negligible in volume relative to the finer grain sizes. Another characteristic feature of the succession is pervasive soft sediment deformation mostly due to vertical foundering (load structures), particularly in the lower to middle part of the Battfjellet Formation but also in the partly interfingering and overlying Aspelintoppen Formation (Steel et al., 1981; Helland-Hansen 2010; Grundvåg et al., 2014b; Naurstad 2014).

Data

Based on field data, our published literature and theses of MSc students we have supervised, thicknesses, paleocurrent data and facies-breakdown have been compiled from logged profiles (c.f. Helland-Hansen, 1985, 1990, 2010; Grundvåg et.al., 2014a,b, and MSc dissertations by Olsen, 2008; Stene, 2009; Gjelberg, 2010; Skarpeid, 2010; Osen, 2012; Naurstad, 2014; Jørgensen, 2015; Kongsgården, 2016; Broze, 2017; Aamelfot, 2019). Figure 1 shows position of the vertical profiles and Figure 4 shows compiled thicknesses and paleocurrent data. For examples of sedimentary logs we refer to Figures 3. and 6 The general facies succession, as well as the detailed depositional architecture of some clinothems is thoroughly documented in previous papers (e.g. Steel, 1977; Helland-Hansen, 1992; Mellere et al., 2003; Johannessen & Steel, 2005; Petter & Steel, 2006; Uroza & Steel, 2008; Helland-Hansen 2010, Grundvåg et al. 2014 a, b) and will not be reiterated here. In the following we will go through individual basin-scale environmental elements moving from continental to offshore and basinal areas, briefly describe their facies development and summarize their spatial distribution as basis for a new regional synthesis of the basin fill history and its controls.

ENVIRONMENTAL ELEMENTS

Coastal plain element

Coastal plain sediments (the Aspelintoppen Formation, Steel et al., 1981; Clifton, 2012; Naurstad, 2014) locally interfinger with and cap the underlying shelf-delta elements (below) and extend all the way to mountain tops (Figure 5a). Depending of the position within the Central Basin and the height of the mountains, the thickness of the Aspelintoppen Formation is highly variable, but as noted above, it may be as much as 1000 m in the central part of the basin (Steel et al., 1981).

Inter-channel floodplain deposits are dominating (Figure 6a, 7a and 7b), but ribbon-shaped channel sandstone bodies a few to maximum 15 m thick with limited laterally extent (tens to a few hundred meters) are variably present (Figure 6a and 7c) (Naurstad, 2014). These are typically single and multiple stacked with erosive, locally conglomeratic bases or internal scours (with frequent mud-clasts and wood fragments) and crude fining upwards and display pervasive soft sedimentary deformation. The channels are interpreted as relatively short-lived low-sinuosity channels (Figure 8) (Naurstad, 2014; Grundvåg et al., 2014b).

Inter-channel floodplain deposits (Figure 6a, 7a and 7b) are dominated by sheet-formed units 0.5–5 m thick. These typically consist of heterolithic deposits grading upwards into very fine to fine-grained sandstones in coarsening- and thickening-upwards units, sometimes interrupted by crude fining-upwards channelized elements 1–3 m thick in medium to very fine-grained sandstones (Figure 7c). The coarsening- and thickening upwards motifs are interpreted in terms of levee and crevasse splay progradation; the fining-upward motifs as crevasse channels (Naurstad, 2014). In addition, 1–5 m thick units of finely laminated mudstones with abundant leaf fragments, siltstones and very fine-grained sandstones as well as thin coal layers (Figure 7a) represent a more quiescent overbank floodplain environment. For detailed facies-breakdown we refer to Grundvåg et al. (2014b) and Naurstad (2014).

According to data from Brogniartfjella in Van Keulenfjorden (cf. Figure 1) the facies pattern of the coastal plain element show remarkably minor gross environmental variations upwards in the succession apart from a relatively limited zone (max. 10 m) in the basal part that shows clear brackish influence (Naurstad, 2014); the remaining upper part being devoid of tidal or brackish water influence. Clifton (2012), in a dissertation about the Eocene flora of Svalbard, studied the same succession at Brogniartfjella and could not find evidence of tidal influence. Grundvåg et al. 2014b recognize facies deposited in brackish-water environments, but identifies no clear tidal signatures in the coastal plain succession in the 50 m cored lower part of the Aspelintoppen Formation in the nearby Sysselmannbreen well (cf. Figure 1). The only exception is bi-directional cross-strata occurring in the up-dip part of some of the shelf-delta parasequences (below) that interfinger with or are encapsulated within the coastal plain facies. These observations are in contrast to previous publications from the same area that have inferred strong tidal influence at multiple levels of the coastal plain system (apparently confined to incised valleys; e.g. Plink-Björklund, 2005), also at the higher stratigraphic levels of the Aspelintoppen Formation.

The system as a whole is suggested to be the result of high subsidence in combination with high sedimentation rates promoting vertical aggradation and frequent channel-avulsion (Naurstad, 2014). The interpreted avulsive nature of the fluvial system is verified and distinctly reflected in the downstream and time-equivalent shelf deltaic deposits in the Battfjellet Formation (see shelf-delta element, below).

Regional distribution of coastal plain element

The regional distribution and thickness of the coastal plain element is primarily a function of the present-day relief of the landscape and the position within the broad syncline of the Central Basin. The thickest preserved successions are present in the axial parts of the Central Basin (Steel et al., 1981) with thinning and eventually absence towards the flanks of the trough. Specifically, the thinning or absence of the Aspelintoppen Formation only reflects modern day erosion; no primary

thinning, pinchout or erosion of the formation has been recorded, apart from smaller scale variations caused by intrinsic sedimentological processes (e.g. localized channel erosion).

Shelf-delta element

Shelf-deltas are typically expressed as a single or repeated shallowing upwards "parasequences" (*sensu* Van Wagoner et al., 1990) grading from mudstones, siltstones and very fine grained sandstones in heterolithic packages up to very fine, fine or medium-grained sandstones (Figure 5b, 5c, 5d, 6 b and 7d) (Helland-Hansen, 2010; Grundvåg et al., 2014b). Individual units often terminate upwards without reaching coastal plain lithosomes, however, exceptions to this occur and the uppermost parasequence will always transition into coastal plain lithosomes as an expression of the change from the marine Battfjellet Formation to the continental Aspelintoppen Formation. The common upwards termination of parasequences in the marine lithosome is an expression of short progradation distance relative to the wedge-out distance of each parasequence beyond the most basinward shoreline position (Figure 9) (Helland-Hansen, 2010). Thickness of individual parasequences ranges from 10–30 meters; where multiple units are stacked, they are separated by marine flooding surfaces (*sensu* Van Wagoner et al., 1990; Figure 5b). The parasequences possess sedimentary structures pointing to tempestite deposition in the lower offshore-transition part of the succession (hummocky-cross-stratification and ball-and-pillow structures) and deposition indicating more continuous wave and shallow-marine current action, locally with tidal influence, in the overlying shoreface to foreshore part of the succession (Figure 7d, 7e an 7f). The latter part is expressed by alternating sets of wave-ripple lamination and plane-parallel lamination passing upwards into low-angle-, through- and planar-cross stratification (Figure 6b; Gjelberg, 2010; Helland-Hansen, 2010). Wave-ripple crests have a broadly N-S orientation across the entire basin (Figure 4d). Occasionally units show tidal influence in the uppermost part (co-sets of bipolar cross-stratification; Figure 6c) or are cut by distributary fluvial systems (upper part of lower parasequence shown in Figure 6b). Detailed facies break-down is given in Helland-Hansen, 2010, and Grundvåg et al., 2014b.

Regional distribution of shelf-delta element

The shelf-delta parasequences are widely distributed across the entire study area. They are conspicuous as the stratigraphically youngest main cliff-forming landscape element in Svalbard, and they constitute volumetrically the most important sand-sink in the basin. At outcrop scale they typically have a horizontal-tabular expression (Figure 5 b, c, d); a result of sand distribution being conditioned by the vertical energy-zonation in the water-column (Figure 9) as opposed to the clinothems of the slope segment that is the result of gravity emplacement *along* dipping bedding planes (below) (Helland-Hansen, 2010). Their progradational distance is typically in the range of 3-6 km and they probably extend less than 20km along depositional strike (Grundvåg et al., 2014b). The number of stacked parasequences is highly variable, also over short (kilometer) distances (Figure 4c), but they seem to be more abundant in the western part of the basin where subsidence rates have been higher and vertical stacking more pronounced. The highly variable number of stacked units points to elongated deltaic lobes that switched laterally as the deltas prograded into and filled the basin. This, in combination with strong evidence of wave agitation suggested by the sedimentary structures, made Helland-Hansen (2010) propose a fluvio-wave interaction type of delta (Figure 8a, b). The parasequences may (Figure 5a, 5d and 5e) or may not extend laterally into shelf-edge and

slope environmental elements, depending on their shelf-transit distance and position in basin; specifically it is only in the western basin-segment parasequences may link up with slope and turbidite lobe elements together constituting large-scale (up to 350 m high) clinothems (cf. Figure 10) (Helland-Hansen, 2010).

Shelf-edge and upper slope element

Stratigraphically, this element is positioned down-dip and seaward of the shelf delta element (above) and up-dip and landward of the slope element (below). The shelf-edge and upper slope element together form up to 5 km long and up to 80 m thick basinward thinning sandstone-dominated wedges or clinothems (see also Helland-Hansen, 1992; Steel et al., 2000; Plink-Björklund et al., 2001; Mellere et al., 2002; Steel and Olsen, 2002; Johannessen & Steel, 2005; Plink-Björklund & Steel, 2005; Pontén & Plink-Björklund, 2009) (Figure 5a, 5d, 5e and 6d).

Internally, the element is characterized by 2–18 m thick coarsening- and thickening-upward successions of alternating thin-bedded mudstones, siltstones and very fine-grained sandstones forming heterolithic sheet-formed units in the lower part passing laterally upward into sharp-based, amalgamated, medium- to thick-bedded, fine- to coarse-grained sandstones (Figure 6d and 6g; Mellere et al., 2002; Plink-Björklund & Steel, 2005; Petter & Steel, 2006). In the lower part of the coarsening-upward units, plane-parallel lamination and current-ripple cross-lamination is common (including climbing sets); locally with abundant soft-sediment deformation (Figure 7g). Individual beds in the upper part are commonly wedge shaped, normally to non-graded, plane-parallel to low-angle laminated, or locally planar cross-stratified, in places forming sigmoidal bars (*sensu* Mutti et al., 1996) 1–2.5 m thick (Grundvåg et al., 2014b). Amalgamated sandstone units, 0.5–3 m thick, incises the sigmoidal bars in places. For detailed facies-breakdown, see Plink-Björklund et al., 2001 and Mellere et al., 2002.

Based on its stratigraphic position, the coarsening- and thickening-upward stacking pattern and the internal facies architecture dominated by traction and current-generated structures, this element is interpreted as fluvial-dominated mouth bars deposited on the shelf-edge and upper slope (Figure 8). Thus, the heterolithic lower segment is interpreted as distal delta front deposits locally extending onto the slope, whereas the more amalgamated upper segment containing sigmoidal bars are interpreted as flood-dominated proximal delta front and mouth bar deposits (Mellere et al., 2002; Grundvåg et al., 2014b).

Slope element

This element contain both mudstone dominated prodelta slope deposits and sandstone dominated slope lobe deposits (distal part of clinothems) (Grundvåg et al., 2014a) and occur downdip and below the shelf-edge and upper slope element (above) and updip and above the flat lying turbidite lobe element (below) (Figure 5a, 5c and 5e).

The prodelta slope deposits occur as a 100–150 m thick interval and comprises mainly laminated, soft-sediment deformed and structureless mudstone to siltstone with subordinate thin-bedded very

fine-grained sandstones (Figure 6e). The sandstone beds are sharp based, normally graded, locally inclined and occasionally contains plane-parallel lamination and current-ripple cross-lamination. Based on its mudstone-dominated character, its stratigraphic position above basin-floor deposits, and by the high frequency of gravity-driven soft-sediment deformed beds (i.e. slumped beds), this facies association is interpreted to represent deposition on a relatively steep prodelta slope (Grundvåg et al., 2014a).

The sandy slope lobe deposits consist of thin- to thick-bedded siltstones and very fine- to fine-grained sandstones that alternates with thin intervals of mudstones, together forming sheet-like bed-sets 2–4 m thick (Figure 6f and 7h). These units stack vertically into basinward-thinning wedges up to c. 20 m thick and 1–3 km long, constituting clinothems which dip basinward with gradients of 2-5° (Figure 4e, 5a and 5e; Mellere et al., 2002; Johannessen & Steel, 2005; Petter & Steel, 2006). Internally, these wedges are coarsening- and thickening-upward or fining- and thinning-upward (Figure 6f). Up-dip toward the shelf-edge, the wedges show a landward increase in both sandstone content and bed-set amalgamation as they pass into the shelf edge and upper slope element (Mellere et al., 2002). The frequency and thickness of interbedded mudstone increases distally, thus forming heterolithic sheet-like deposits on the lower slope and proximal basin floor (Plink-Björklund & Steel, 2005). Still, at some localities (e.g. Storvola, cf. Figure 1) the sandy slope lobes can be traced basinward and down-dip into the turbidite lobes (Figure 5a and 5e) within the basin floor element (below) (Crabaugh & Steel, 2004; Petter & Steel, 2006).

The coarsening - and thickening-upward or fining- and thinning-upward is recording progradation and retrogradation or lateral switching of slope lobes, respectively (Petter & Steel, 2006). The landward increase in sandstone content and bed-set amalgamation, and the up-dip transition into fluvial-dominated mouth bars, suggests that the lobes were fed by shelf-edge deltas (e.g. Mellere et al., 2002; Petter & Steel, 2006). Sandy slope lobe deposits have been discussed in more detail by Steel et al. (2000), Plink-Björklund et al. (2001), Mellere et al. (2002), Plink-Björklund & Steel (2005) and Petter & Steel (2006).

In addition, lens-shaped, erosionally based, thin-to thick-bedded fine- to coarse-grained sandstone bodies encapsulated within thicker mudstone intervals occurs within this element (Figure 6g and 7i). The sandstone bodies are typically 4–10 m thick, and depending on outcrop orientation 50–300 m wide, and pinches out both landward and basinward (Johannessen & Steel, 2005). Internally, some of the bodies are thin- to medium bedded and contain lateral accretion surfaces, but more commonly they are thick-bedded and amalgamated (Figure 7i; see also Johannessen & Steel, 2005), contain mud chips conglomerates, and flute casts. Based on the erosive bases and lens-shaped geometries, and its stratigraphic position in a prodelta slope setting above turbidite lobes, these are interpreted as middle to lower slope channels (Johannessen & Steel, 2005). Slope channels have earlier been described in the south-eastern part of the study area by Johannessen & Steel (2005), Clark & Steel (2006), and Petter & Steel (2006).

Regional distribution of shelf-edge and slope element

Shelf-edge and slope deposits are most evident in the western part of the basin where they readily can be identified as sandstone clinothems protruding downwards through finer grained sediments (Figure 4e). Gradients, when restored for tectonic tilt, range from 2-5°, and their relief from 150 m to 250 m (Plink-Björklund et al., 2001; Mellere et al., 2002; Petter & Steel, 2006). Albeit conspicuous

features, the sandstone clinothems only constitutes a minor part of the slope element; slope deposits are generally mudstone and siltstone dominated (Figure 6g and 10; Grundvåg et al., 2014a) in the western segment of the basin and entirely dominated by fine-grained material in the eastern segment (Figure 10). In outcrops the fine material will normally be scree-covered, but well data in both the western (Grundvåg et al., 2014a) and eastern parts (Osen, 2012) of the basin confirms the dominance of fine-grained material. Despite this mudstone-dominance, the presence of sandstone clinothems (and basin floor turbidite lobes, below) restricted to the western part of the basin (Figure 4e and 4f) is a clear expression of deep water and steep slopes in this part of the basin providing potential energy for mass-gravity processes (Helland-Hansen, 1992; 2010). The sandy channels that are also present within the slope element further demonstrates the importance of transport of sandy material from shelf-edge deltas to the basin floor (Johannessen & Steel, 2005).

Basin floor element

The basin floor element is dominated by a finely laminated mudstone succession, but also includes 2–10 km long and up to 60 m thick basinward thickening-thinning sandstone wedges (Figure 6 h, i; Crabaugh & Steel, 2004; Grundvåg et al., 2014a). These have a markedly lower depositional gradient than their associated and partly up-dip connected sandy slope lobe counterparts (Figure 5a and 5e). The wedges comprise alternating siltstone, heterolithic units and thin- to thick-bedded very fine- to medium- and subordinate coarse-grained sandstones (Figure 7j). The sandstone beds are generally normally graded, records basinward thinning and -fining, and occur as vertically stacked coarsening- and thickening-upward units, 1–12 metres thick, with sheet-like geometries (Grundvåg et al., 2014a). Individual units are typically separated by siltstones or heterolithic intervals (Figure 6 h and 6i). Locally, erosionally based, amalgamated thick-bedded sandstone units typically cap or incise the coarsening- and thickening-upward units (e.g. upper part of succession shown in Figure 6h; Grundvåg et al., 2014a). Basinward, the sheet-like units grades into heterolithic deposits. Detailed facies breakdown is given in Grundvåg et al., 2014a.

The sandstone-dominated part of this element is interpreted as gravity-emplaced sandy deposits forming channelized turbidite lobe-complexes on the otherwise mudstone-dominated lower slope and basin floor (e.g. Crabaugh & Steel, 2004; Clark & Steel, 2006). Normally-graded sandstone beds that fine and thins basinward and locally comprises current-generated structures, indicates deposition from down-slope decelerating turbidity currents. Stacked coarsening- and thickening-upward successions represent prograding lobes and lobe elements (e.g. Prélat et al., 2009; MacDonald et al., 2011). The heterolithics located basinward of these successions represent the lobe fringe (e.g. Hodgson et al., 2006).

Regional distribution of basin floor element

As for the slope element, the sandstone dominated parts of the basin floor element only has a clear outcrop expression in the western segment of the basin (Figure 4f and 10). In Nathorst Land, turbidite lobe deposits apparently occur in two distinct zones trending NNW-SSE across the entire peninsula; the westernmost of these zones can be extended northwards to Nordenskiold Land (Figure 4f). Each zone is approximately 7–9 km wide and is present in the western and central parts of the basin. The easternmost limit of these deposits coincides with the eastern limit for the

presence of sand-prone shelf-margin clinothems (Figure 4e), thus confirming the link between shelf-edge deltas and deep-water deposition (cf. Johannessen and Steel, 2005; Helland-Hansen, 2010). It might be speculated that the two documented zones with turbidite lobe deposits represent two pronounced episodes with basin-wide bypass of sand-grade sediments to the basin floor. In other foreland basins similar basin-floor gravity flow deposition have been interpreted to reflect deposition following periods of tectonically-induced hinterland uplift (e.g. Mutti et al., 2003).

The basin floor sandstones are all encased in mudstones and siltstones (basin floor below, prodelta slope above) that less commonly crop out. In the eastern part of the basin, thicker basin floor sandstone elements are not evident in outcrops. This could partly be due to scree cover; however, well data in this region are devoid of turbidite lobe deposits supporting the notion of their absence in this area (Osen, 2012).

Deepwater shale element

Below the level of the basin floor turbidite lobes and down to the top of the Hollendardalen Formation in the western part of the basin and the Grumantbyen Formation further east (beyond the eastward pinchout of the Hollendardalen Formation, Figure 2), monotonous shales dominates, with thicknesses of about 300-370m in the western part of the basin (cf. well BH 10-2008, Sysselmannsbreen well, Grundvåg et al., 2014a; see also Steel et al., 1981). In the eastern part of the basin it is more difficult to estimate these thicknesses because basin floor deposits time equivalent to the turbidite lobe deposits in the western part of the basin are here mudstone dominated and hence, a datum for estimating sub-basin floor element shale thicknesses is missing. Wells in the eastern part of the basin, west of Svea (BH 11-2003 and BH 10-2006), have shale thickness (from top Grumantbyen Formation to base Battfjellet Formation) ranging from 340 to 370 m (cf. Figure 10) (Osen, 2012), which is in the same order as the shale thickness *below* the turbidite lobes of the basin floor element in the Sysselmannbreen well (BH 10-2008) at Nathorst Land (Grundvåg et al., 2014b).

Facies-wise the mudstones are organic rich (total organic carbon 3%, Harding et al., 2011) and finely laminated (Figure 7k). They contain rare pin-striped laminations of siltstone, and concretions and siderite bands are common (Figure 7k). Siltstones and thin sandstones are increasing in frequency upwards towards the basin floor element. The deposits reflect tranquil background deep-water pelagic or hemi-pelagic sedimentation out of reach from high-energetic processes (Grundvåg et al., 2014a).

BASIN FILL OVERVIEW

Linkage of environmental elements

Figure 10 shows a cross-sectional representation of the facies elements discussed above in their relative stratigraphic position. Generally, the progradational GBA-unit shows a shingled time transgressive architectural pattern of coastal plain to marine lithosomes all over the basin. As noted, individual shelf-delta parasequences generally show a tabular geometry at outcrop scale, an

expression of a sand distribution being conditioned by the vertical energy-zonation in the water-column (Figure9) (Helland-Hansen, 2010).

It is these parasequences that in the western basin-segment in a few instances are seen to peel off into discernible slope- and sometimes also basin floor turbidite lobes (Figure 5a, 5d, 5e and 10). Hence, both shelf-edge element, sandy slope element (together constituting clinothems) and turbidite lobes of the basin floor element are restricted to the western part of the basin (Figure 4e and 4f). As pointed out in earlier publications (e.g. Helland-Hansen, 1990, 2010) this reflects deeper water in the western basin-segment fostering steeper gradients and more potential energy for mass transport processes to funnel sediments beyond the "littoral energy fence" and into deeper water as opposed to the eastern segment where shallower waters persisted.

This west-east distinction is also expressed in the thickness map of the marine part of the Central Basin foredeep succession (combined Hollendardalen Formation and GBA-unit, Figure 4b); a clear westward thickening emphasizes the asymmetrical downwarping in front of the fold-and-thrust-belt. However, as can be speculated from the apparently relative uniform thickness of the deep water shale element across the basin (below the basin-floor-turbidite-lobes in the western part of the basin, Figure 10), this downwarping may have been most pronounced in the later stage of the marine basin fill, specifically from the time of initiation of turbidite lobe deposition and onwards. Some uncertainty is attached to defining the sub basin floor thickness in the eastern part of the basin since the basin floor element here is not clearly expressed. Still the lack of sandstone clinothems and turbidite lobes in this part of the basin points to shallower water than in the west during this stage of basin development with water depths more likely in the order of tens of meters. A development in compliance with the numerical models of Flemings & Jordan (1989) can be envisaged. They demonstrated an early thrust-sheet emplacement phase causing asymmetric subsidence towards the orogen (with only minor shoreline progradation), followed by shoreline progradation into the foredeep during post thrust-load-emplacement isostatic uplift. A similar two-stage tectonostratigraphic development can be inferred for the Hollendardalen Formation (Figure 2) which shows a similar westerly thickening as the above-mentioned part of the GBA-unit.

The predominance of fine material in the GBA-unit as a whole (dominantly mudstones, siltstones and very fine- and fine-grained sandstones) with virtually lack of conglomeratic material is a characteristic feature of the basin fill. Even within the most proximal coastal plain element (the Aspelintoppen Formation) only the very basal parts of fluvial distributary channels include some conglomeratic material (Naurstad, 2014) and no sourceward increase in grain size is recorded. This suggests that coarser grained material was extracted closer to the source area beyond the current outcrop limits or, alternatively, that the source area did not yield coarser material which may seem likely owing to predominance of Late Paleozoic and Mesozoic rocks in the source area (cf. Petersen et al., 2016.). Nonetheless, from this it can be inferred that more proximal continental depositional environments (e.g. potential braidplains and alluvial fans) were still some distance away at the time of coastal plain deposition of the Aspelintoppen Formation across the area.

Trajectory

The system as a whole demonstrates a gradually ascending shelf-edge trajectory with successive shelf-edge and shelf deltas occupying successively stratigraphically higher positions as the system builds into the basin (cf. Deibert et al., 2003; Løseth et al., 2006) (Figure 10). The overall ascending trajectory is punctuated by transgressive events (Figure 10), of which most are interpreted to be the effect of delta lobe shifting (Helland-Hansen, 2010). Grundvåg et al. (2014b) calculated the average trajectory to be 0. 88° and 1.2°, based on correlations of the Battfjellet Formation along the south side of Van Mijenfjorden (36.5 km long transect) and north side of Van Keulenfjorden (22 km long transect) respectively. The thick succession of continental deposits of the Aspelintoppen Formation, 1 km maximum preserved thickness and in the order of ½ km removed (Marshall et al., 2015), indicates that the shorelines in front of the coastal and alluvial plains were climbing stratigraphically beyond the preserved limits of the basin, further to the east and possibly also to the south (see discussion below).

DISCUSSION - CONTROLS ON BASIN FILL

Basin type

The GBA-unit was laid down in the foredeep zone of a foreland basin system (sensu DeCelles and Giles, 1996) as evidences by (i) the pronounced thickening of the succession towards the orogeny and (ii) the absence of intraformational unconformities or progressive deformation.

Syndepositional thrusting along decollement zones in the underlying Late Paleozoic and Mesozoic succession (Braathen & Bergh, 1995; Blinova et al., 2013) may have transformed the basin into a wedge-top basin in later stages of the basin filling. E.g. Blinova et al., 2013 indicates development of a decollement zone within Triassic shales contemporaneous with intense Eocene transpression; movement along this zone is likely to have coincided in time with basin filling. The pronounced westward thickening of the upper marine part of the succession (Figure 4b) points to a foredeep rather than a wedge-top setting, however, it cannot be excluded that the transformation into a wedge-top basin took place contemporaneous with the deposition of the continental Aspelintoppen Formation or during deposition of the sediments that have later been eroded. Gentle structuring on the basin floor producing swells and troughs may have formed already during the emplacement of the basin floor fans. This is suggested by apparent north to northeastward-directed palaeocurrent indicators (i.e. flute casts and tool marks) in some of the submarine fan bodies (Crabaugh & Steel, 2004). Alternatively, this may be explained in terms of increased lateral spreading of turbidity flows as they move across an unconfined basin floor (cf. large spread in palaeocurrent directions in eastern part of basin, Figure 4f).

The Svalbard foreland basin is anomalous in the sense that it is bordered by a transpressive orogeny and is such classified as a transpressional basin (Ingersoll, 1988). Transform movements is evidenced by the regional picture as well as the present structural configuration (Steel et al., 1985; Faleide et al., 1993; Bergh & Grogan, 2003; Faleide et al., 2008; Dore et al., 2015; Kristensen et al., 2018). The predominantly western input recorded in the succession strongly reflects ongoing shortening and uplift in the west; however, evidence of strike-slip in the sedimentary succession, such as lateral

519 migration of depocenters and lateral offsets of matched provenance areas and deposits (Nilsen &
520 Sylvester, 1999), has not been demonstrated. The absence of evidence for the strike-slip regime in
521 the succession could simply be an expression of the length of the studied segment of the foreland
522 basin relative to the full strike extent of the orogeny, preventing signs of strike-slip to be recorded in
523 the sedimentary succession.

524 An integral part of foreland basins is the peripheral bulge (DeCelles and Giles, 1996). We suggest that
525 the thinning we see towards the east is an expression of deposition on the flank of the peripheral
526 bulge. There is no evidence to suggest that the bulge was elevated above sea-level since neither
527 regional erosion and/or reversal of sediment routing is evident in the more distal part of the
528 succession (cf. Bruhn & Steel, 2003).

529 The present day Hornsund Fault Zone off the Svalbard margin, about 50km west of the present day
530 Central Basin axis, may have been close to the axis of the shear-zone between Greenland and
531 Svalbard (Eldholm et al., 1987) and it is reasonable to assume that the drainage divide was not
532 located west of this. Hence, the source area was probably relatively close to the basin. From
533 established scaling relationships between drainage area and catchment length (Hack, 1957; Helland-
534 Hansen et al., 2017), we assume that the catchments that fed the foreland basin was relatively small;
535 500–1000 km^2 (Figure 8).

536

537 **Basin forming processes**

538 The thickness (maximum a few kms) and width (few tens of kms) of the Svalbard foredeep succession
539 is moderate relative to what is typical for compressional foredeep depozones (typically 2–8 km thick
540 and 100-300km wide, DeCelles & Giles 1996). The anomalous low thickness and width may be typical
541 for transpressional foredeeps; these are normally less than 100 km wide (c.f. de Urreiztieta et al.,
542 1996; Eichhubl et al., 2002; Meng et al., 2005). A factor that may play a role in defining the limited
543 width and amplitude of the transpressional foredeeps could be shearing along the transform margin
544 partitioning the crust also within the foredeep zone. The main effect of lateral change in the
545 lithosphere, such as disruptions by strike-slip motions, would be to increase the amplitude of the
546 basin at the expense of reducing the width (Beamount et al., 1982).

547 Alternatively, the shallow depth and short wave-length could be an expression of basin-formation by
548 crustal buckling rather than flexural downwarping. Zhang & Bott (2000) proposed a model of plastic
549 compressional folding as an alternative to the supracrustal loading model for foreland basin
550 development. However, both their modelling results and the basins they refer to that supports their
551 modelling experiments all have much deeper basins than what is recorded in the Svalbard foredeep.
552 Criteria to identify flexural loading includes a significant depth and thickening of foreland basin
553 successions close to the thrust front and accompanying rapid tapering towards the craton and minor
554 amplitudes in deflection beyond the forebulge. Buckling on the other hand tends to form repeated
555 gentle anticlines and synclines at long distances (>>1000km) away from the orogeny (Allen & Allen,
556 2013).

557 Although these considerations are based on settings of pure compression and not necessarily directly
558 applicable to transpressive settings, we believe that the pronounced thickening of the basin fill

559 towards the orogeny (Figure 7b) is an expression of dominance of downflexing rather than buckling.
560 However, thin-skinned partitioned shortening involving buckling cannot be excluded as an additional
561 process. The thickness map of the Central Basin foredeep succession (Figure 4b) demonstrates NW-
562 SE trending isopachs with thickening towards the SW. This trend is oblique to the present NNW-SSE
563 structural grain of the WSFTB and could be an expression partitioned shortening related to the right-
564 lateral oblique motions along the margin (cf. Sanderson & Marchini, 1984). This is also in agreement
565 with the Eocene NE-SW crustal shortening proposed by Braathen et al., 1999 (their stage 4-5). It
566 should be noted that Kristensen et al. (2018) demonstrated a depocenter oblique to the sheared
567 margin in the Sørvestsnaget Basin along the Senja Shear Margin (Figure 1), a southwards extension of
568 the Svalbard Margin in the Barents Sea. This depocenter also have an Eocene infill with a similar
569 counter-clockwise isopach obliquity (20-30°) to the Senja Shear Margin as the Central Basin foredeep
570 succession has to the Svalbard Margin. However, this basin is much narrower (ca. 5 km, Central Basin
571 ca. 50km) and is related to crustal buckling associated with a transtensional regime (Kristensen et al.,
572 2018).

573 The presumably maximum removed overburden in the Central Basin based on vitrinite reflectance
574 data in the coals of the Firkanten Formation (Manum & Throndsen, 1978; cf. also Marshall et al.,
575 2015) coincides with the present axis of the Central Basin. Hence, the depocenter of the
576 Aspelintoppen Formation and eroded deposits is eastwards offset not only to the marine part of the
577 GBA-unit, but also relative to the depocenter of the older Paleogene formations (cf. Bruhn & Steel,
578 2003) and may point to an eastward and cratonward migrating depocenter (Helland-Hansen 1990).

579

580 **Subsidence and eustasy**

581 Dörr et al., 2013 performed a backstripping and subsidence analysis of the post-Devonian
582 sedimentary succession of Svalbard. In their one-dimensional backstripping they arrived at an
583 average subsidence rate (including isostatic and compactional subsidence) for Van Mijenfjorden
584 Group at 0.04mm/yr (1 km over 25 my, cf. their Figure 4). It is reasonable to suggest that subsidence
585 rates were significantly higher than average during the deposition of the upper marine succession
586 (from level of basin floor turbidite lobes and through the Battfjellet Formation and time-equivalent
587 Aspelintoppen Formation deposits) due to significant downflexing of the crust associated with the
588 climax of the WSFTB.

589 We compared the average subsidence rate of Dörr et al., 2013 with rates derived from the eustatic
590 sea-level curve of Miller et al., 2005 for the Eocene. Several major falls have rates exceeding 0.04
591 mm/yr, included the very pronounced early Eocene (52, 8–51 my) eustatic fall with an amplitude of
592 79 m and an average fall-rate of 0,044mm/yr. At least 5 longer periods within the Eocene have
593 significant sea-level falls with average rates exceeding 0.04mm/yr. Maximum rates for 100 000 year
594 periods exceeds 0.1mm/yr 16 times. However, one should keep in mind the gravitational attraction
595 that the supracrustal load of the WSFTB exerted on the sea-level; this would cause higher than
596 average sea-level and hence, subdued effect of potential eustatic sea-level falls (cf. Haq, 2014)

597 The question is whether potential relative sea-level falls can be identified in the studied succession.
598 Several papers have suggested repeated episodes of relative sea-level falls (frequently below shelf-
599 edge) (Plink-Björklund et al., 2001; Plink-Björklund & Steel, 2002; Mellere et al., 2002), and interpret

incised valleys from sedimentological criteria (Mellere et al., 2003; Plink-Björklund, 2005; Plink-Björklund & Steel, 2006). For example, Plink-Björklund & Steel (2006) identified three incised valleys within the coastal plain succession (i.e. the Aspelintoppen Formation) at Brogniartfjella (location in Figure 1) with an estimated fluvial downcutting of 26 m, 57 m and 67 m, respectively. The two deeply cut valleys apparently resulted from relative sea-level falls below the shelf edge, eventually resulting in slope bypass and the development of coeval basin-floor fans (Plink-Björklund & Steel, 2006). In addition, the same authors interpret subaerial unconformities and associated wave-cut terraces on the upper part of the Högsnyta slope wedge (location in Figure 1), again advocating fall of sea level below shelf edge (Plink-Björklund & Steel, 2002). Grundvåg et al., 2014b on the other hand, states that there is no clear evidence of any significant basinward facies dislocations or erosional unconformities within the Battfjellet Formation based on data from Nathorst Land (including Brogniartfjella, see Figs. 9 and 11 in Grundvåg et al., 2014b). Grundvåg et al. (2014b), do however, recognize the presence of erosively-based distributary channel fills cut down into their associated delta front facies, and incised upper slope to shelf-edge channel complexes whose origin is debatable (e.g. retrogressive slumping, see Steel et al., 2000). Relative sea-level falls imply significant eustatic falls to counteract the typically high rates of foreland basin subsidence (cf. Allen and Allen, 2013). Literature discussing relative sea-level changes within the foredeep zones generally favour absence of relative sea falls: subsidence rates in foreland basins has been argued to invariably exceed the rate of eustatic falls in areas proximal to the orogenic belt, but only sporadically in regions distal to the thrust load (Posamentier and Allen, 1993; Willis, 2000; Castle, 2001; Hoy and Ridgway, 2003; Escalona & Mann, 2006; Bera et al., 2008).

As noted above, a major element in the basin filling style is the shingled appearance of the coastal plain to shallow marine lithosomes and the highly variable number of shelf-deltas over short distances (Figure 4c and 10). This has been attributed to an elongate morphology of the deltas with pronounced delta-lobe shifting, each lobe-shift and accompanying flooding producing intervals of fine-material deposition (Helland-Hansen, 1992; Grundvåg et al., 2014b). Still, it can be questioned whether all finer-grained levels (typically separating the cliff-forming sandstones) should be attributed to lobe-shifting. Some fine-grained units are seen to produce thicker and more laterally extensive ledges along the mountainsides and may represent events of relative sea-level rise of more widespread nature than what can be produced from more local flooding events emanating from shifting of delta-lobes. In light of the proposed high subsidence rates in combination with recurrent eustatic sea-level rises it seems easier to argument for major events of relative sea-level rise than for relative sea-level fall.

Sediment supply

Sediment was primarily derived from the west as evidenced by paleocurrent data across the basin as well as the direction of sloping and thinning of clinothems in the western part of the basin (Figure 4e and 4f). In addition, provenance studies confirm a western source area for the GBA-unit (e.g. Petersen et al., 2016). Notable is the nearly uniform N-S orientation of wave ripple crests across the basin (Figure 4d) and current generated structures at the delta front and basin mostly have easterly directions (Figure 4e and 4f) (Helland-Hansen, 1990; Grundvåg et al., 2014b). Wave-ripple crests typically align parallel to the coast (Potter & Pettijohn, 1963) and correspond well with the easterly

directed current generated structures and the eastwards sloping clinoforms, together indicating eastwards advancing deltas.

The west to east transport direction is oblique to the NW-SE isopach trend. Isopachs in overfilled basins (Hadler-Jacobsen et al., 2005) reflect long term spatial variations in subsidence. However, progradational elements of such systems, in this case delta progadation, may simply "ignore" slow and long-term subsidence and subsidence-variations simply from the fact that progradation across the basin is a rapid process compared to subsidence. Tectonic basin subsidence is <0.5mm/yr for most basin types (Allen & Allen, 2013) whereas delta progradation is a measure of meters to hundreds of meters per year (Aadland & Helland-Hansen, 2016), explaining the mismatch between transport directions and isopach trends.

Several sedimentological criteria indicate temporally high sedimentation rates. The pervasive soft sediment deformation at multiple levels (Steel et al., 1981; Helland-Hansen 2010; Grundvåg et al., 2014b; Naurstad 2014), and in particular in heterolithic successions, points to rapid deposition, subsequent dewatering and accompanying deformation. Much of this soft sediment deformation is seen to be caused by vertical foundering rather than lateral down-slope movement (evidenced by predominance of ball-and-pillow and other loading structures relative to structures caused by slumping) (Helland-Hansen, 2010; Grundvåg et al., 2014b). The lower heterolithic part of the Battfjellet Formation, the heterolithic (inter-channel) successions in the Aspelintoppen Formation and fluvial sandbodies in the Aspelintoppen Formation are the levels with most frequent soft sediment deformation structures. In the slope wedges, the abundance of thick-bedded hyperpycnal turbidite beds rich in plant material indicate the presence of high-supply shelf-edge deltas (Plink-Björklund & Steel, 2004). The high degree of bed amalgamation in the turbidite lobes, as well as their progradational stacking also indicates a high supply system (Grundvåg et al., 2014a). In addition, the immature character of the sediment with poor sorting and abundance of unstable fragments (including organic detritus and shale fragments) (cf. Helland-Hansen, 2010) suggests rapid deposition and little time for winnowing of sediments, even in the shallow marine domain.

Basin extent

How far south and east did the basin extend? It is known from seismic studies in the western and SW Barents Shelf that a large middle Eocene-Oligocene clinoform system shed significant amounts of sediments into the deeper parts of the Vestbakken Volcanic Province and the Sørvestsnaget Basin (cf. Figure 1) (e.g. Rasmussen et al., 1995; Ryseth et al., 2003; Safronova et al., 2014; Lasabuda et al., 2018). Specifically, Safronova et al. 2014 reported southwards prograding clinoform systems of middle Eocene age in the Sørvestsnaget Basin and proposed that these were sourced from the Stappen High. The latter feature was uplifted in the Early Eocene as a response first to shearing and later rift flank uplift as this segment of the Northernmost Atlantic separated from the Greenland margin (Gabrielsen et al., 1990). It is likely that the Stappen High was connected to the WSFTB and that a coastline run from the Central Basin and southwards to the eastern flank of the Stappen High (Bergh & Grogan, 2003). According to Smelror et al. (2009) this sea was narrow in the Svalbard area extending south with its eastern shores in the immediate vicinity of the present day eastern margin of the Central Basin. Further south, towards 76°N, the sea is indicated with an eastern branch. We believe that his sea extended much further eastwards also in the Central Basin area. The overweight

of eastward directed paleocurrent directions in the GBA-unit throughout the basin, suggests that the drainage did not orient southwards during the time encompassed by the preserved marine and continental infill. However, it should be noted that paleocurrent data in fluvial channel-fills of the Aspelintoppen Formation commonly have southeasterly directions, which may indicate early clockwise rotation of drainage patterns (cf. Figure 7c). Potential feeding of sediments to the western and SW Barents Shelf would have been routed farther east and southeast and beyond the present day Central Basin eastern margin before turning south. A possible peripheral bulge east of the present Central Basin margin may have been instrumental in this southwards sediment diversion. Although speculations, a southwards sediment transport may also have been important along the Central Basin during the deposition of the younger foreland basin fill that later was eroded.

CONCLUSIONS

The post early Eocene Gilsonryggen Member, Battfjellet Formation and Aspelintoppen Formation together formed an eastwards prograding megasequence (> 1km thick) filling the foreland of the West Spitsbergen fold-and-thrust belt. The catchments were small (500–1000 km^2) and the distance to the source terrain and probably also the drainage divide was short (< 100km). The succession consists of coastal plain, shelf delta, shelf-edge, slope, basin floor and deepwater shale elements with shelf-edge deltas, slope clinothems and basin floor fans being restricted to the western and deepest part of the basin. The system prograded with an ascending trajectory around 1° and it is expected that this trend also persisted beyond the preserved outcrop belt, explaining the considerable thickness (> 1km) of the continental deposits capping the progradational package. The progradational architecture demonstrates an extremely shingled character with limited lateral extent (3-6 km) of basinward offset shallow-marine lithosomes. The sediment supply rate was temporarily high as evidenced by immaturity of the rocks and the pervasive soft sediment deformation and probably is a reflection of the proximity to the source area. Sediments accumulated in a foredeep zone of a foreland basin system with subsidence driven by flexural loading potentially accompanied by crustal buckling. From the high-subsidence foredeep setting it can be assumed that subsidence outpaced eustatic sea-level falls and that episodes of relative sea-level falls were few. The system may have been connected to contemporaneous progradational systems west and south of the Stappen High further south, however, evidence of southwards sediment routing is not evident in the system.

REFERENCES

Aadland, T. & Helland-Hansen, W. (2016). Global compilation of coastline change at river mouths. In: *EGU General Assembly Conference Abstracts*, *18*, pp. 3915.

Aamelfot, T. (2019). *Sedimentology of the Battfjellet Formation, Liljevalchfjellet, Svalbard*. MSc thesis, University of Bergen, Norway, 102 pp.

Allen, P.A. & Allen, J.R. (2013). *Basin analysis: Principles and application to petroleum play assessment*. John Wiley & Sons, Hoboken, 327 pp.

Atkinson, D.J. (1963). Tertiary Rocks of Spitsbergen. *American Association of Petroleum Geologists Bulletin, 47*, 302-323.

Beaumont, C., Keen, E. & Boutilier, R. (1982). A comparison of foreland and rift margin sedimentary basins. *Philosophical Transactions of the Royal Society of London, A, 305*, 295-317.

Bera, M., Sarkar, A., Chakraborty, P., Loyal, R. & Sanyal, P. (2008). Marine to continental transition in Himalayan foreland. *Geological Society of America Bulletin*, *120*, 1214-1232.

Bergh, S.G. & Grogan, P. (2003). Tertiary structure of the Sørkapp-Hornsund Region, South Spitsbergen, and implications for the offshore southern extension of the fold-thrust Belt. *Norwegian Journal of Geology*, *83*, 43-60.

Bergh, S.G., Braathen, A. & Andresen, A. (1997). Interaction of basement-involved and thin-skinned tectonism in the Tertiary fold-thrust belt of central Spitsbergen, Svalbard. *American Association of Petroleum Geologists Bulletin*, *81*, 637-661.

Birkenmajer, K. & Narebski, W. (1963). Dolerite drift blocks in marine Tertiary of Sørkapp Land and some remarks on the geology of the eastern part of this area. *Norsk Polarinstitutt Årbok*, *1962*, 68-79.

Blinova, M., Faleide, J.I., Gabrielsen, R.H. & Mjelde, R. (2013). Analysis of structural trends of sub-sea-floor strata in the Isfjorden area of the West Spitsbergen Fold-and-Thrust Belt based on multichannel seismic data. *Journal of the Geological Society*, *170*, 657-668.

Braathen, A. & Bergh, S.G. (1995). Kinematics of Tertiary deformation in the basement-involved fold-thrust belt, western Nordenskiold Land, Svalbard: Tectonic implications based on fault slip data analysis. *Tectonophysics, 249*, 1–29.

Braathen, A., Bergh, S.G. & Maher, J.H.D. (1999). Application of a critical wedge taper model to the Tertiary transpressional fold-thrust belt on Spitsbergen, Svalbard. *Geological Society of America Bulletin, 111*, 1468-1485.

Broze, E. (2017). *The occurrence of flow transformations within sandy submarine fans: A case study from the Eocene on Spitsbergen.* MSc thesis, University of Tromsø, Norway, 147pp.

Bruhn, R. & Steel, R. (2003). High-Resolution Sequence Stratigraphy of a Clastic Foredeep Succession (Paleocene, Spitsbergen): An Example of Peripheral-Bulge-Controlled Depositional Architecture. *Journal of Sedimentary Research, 73*, 745-755.

Castle, J.W. (2001). Foreland-basin sequence response to collisional tectonism. *Geological Society of America Bulletin, 113,* 801-812.

Charles, A.J., Condon, D.J., Harding, I.C., Pälike, H., Marshall, J.E.A., Cui, Y., Kump, L. & Croudace, I.W. (2011). Constraints on the numerical age of the Paleocene-Eocene boundary. *Geochemistry, Geophysics, Geosystems*, *12*, 1-19.

Clark, B.E. & Steel, R.J. (2006). Eocene turbidite-population statistics from shelf edge to basin floor, Spitsbergen, Svalbard. *Journal of Sedimentary Research, 76*, 903-918.

Clifton, A. (2012). *The Eocene flora of Svalbard and its climatic significance.* PhD thesis, University of Leeds, UK, 401pp.

Crabaugh, J.P. & Steel, R.J. (2004). Basin-floor fans of the Central Tertiary Basin, Spitsbergen; relationship of basin-floor sand-bodies to prograding clinoforms in a structurally active basin. In S.A. Lomas & P. Joseph (Eds.), *Confined Turbidite Systems* (Vol. *222*, pp. 187-208). London, Geological Society, Special Publications.

Dalland, A. (1977). Erratic clasts in the Lower Tertiary deposits of Svalbard—evidence of transport by winter ice. *Norsk Polarinstitutt Årbok 1976*, pp. 151-165

Dallmann, W.K. (1999). *Lithostratigraphic Lexicon of Svalbard.* Committee on the Stratigraphy of Svalbard/Norsk Polarinstitutt, Tromsø, 318 pp.

Dallmann, W.K. & Elvevold, S. (2015). Bedrock Geology. In: *Geoscience Atlas of Svalbard* (Ed. W.K. Dallmann), *Norwegian Polar Institute, Report Series, 148*, 133-173.

DeCelles, P.G. & Giles, K.A. (1996). Foreland basin systems. *Basin Research*, *8*, 105-123.

Deibert, J.E., Benda, T., Løseth, T., Schellpeper, M. & Steel, R.J. (2003). Eocene Clinoform Growth in Front of a Storm-Wave-Dominated Shelf, Central Basin, Spitsbergen: No Significant Sand Delivery to Deepwater Areas. *Journal of Sedimentary Research, 73*, 546-558

De Urreiztieta, M., Gapais, D., Le Corre, C., Cobbold, P. & Rossello, E. (1996). Cenozoic dextral transpression and basin development at the southern edge of the Puna Plateau, northwestern Argentina. *Tectonophysics*, *254*, 17-39.

Dimakis, P., Braathen, B.I., Faleide, J.I., Elverhøi, A. & Gudlaugsson, S.T. (1998). Cenozoic erosion and the preglacial uplift of the Svalbard–Barents Sea region. *Tectonophysics*, *300*, 311-327.

Doré, A.G., Lundin, E.R., Gibbons, A., Sømme, T.O. & Tørudbakken, B.O. (2015). Transform margins of the Arctic: a synthesis and re-evaluation. In M. Nemcok,, S. Rybar, S.T. Sinha, S.A. Hermeston & L. Ledvenyiova (Eds.), *Transform Margins: Development, Controls and Petroleum Systems* (Vol. *431*, pp. 63-94). London, Geological Society, Special Publication,

Dörr, N., Clift, P.D., Lisker, F. & Spiegel, C. (2013). Why is Svalbard an island? Evidence for two-stage uplift, magmatic underplating, and mantle thermal anomalies. *Tectonics*, *32*, 473-486.

Eichhubl, P., Greene, H.G. & Maher, N. (2002). Physiography of an active transpressive margin basin: high-resolution bathymetry of the Santa Barbara basin, Southern California continental borderland. *Marine Geology*, *184*, 95-120.

Eldholm, O., Sundvor, E., Myhre, A.M. & Faleide, J.L. (1984). Cenozoic evolution of the continental margin of Norway and western Svalbard. In A.M. Spencer (Ed.), *Petroleum Geology of the North European Margin* (pp. 3–18). London, Graham & Trotman.

Eldholm, O., Faleide, J.I. & Myhre, A.M. (1987). Continent-ocean transition at the western Barents Sea/Svalbard continental margin. *Geology*, *15,* 1118-1122.

Escalona, A. & Mann, P. (2006). Sequence-stratigraphic analysis of Eocene clastic foreland basin deposits in central Lake Maracaibo using high-resolution well correlation and 3-D seismic data. *American Association of Petroleum Geologists Bulletin, 90*, 581-623.

Faleide, J.I., Vågenes, E. & Gudlaugsson, S.T. (1993). Late Mesozoic–Cenozoic evolution of the southwestern Barents Sea. *Geological Society, London, Petroleum Geology Conference Series*, *4*, 933-950.

Faleide, J.I., Tsikalas, F., Breivik, A.J., Mjelde, R., Ritzmann, O., Engen, O., Wilson, J. & Eldholm, O. (2008). Structure and evolution of the continental margin off Norway and the Barents Sea. *Episodes*, *31*, 82-91.

Flemings, P.B. & Jordan, T.E. (1989). A synthetic stratigraphic model of foreland basin development. *Journal of Geophysical Research - Solid Earth*, *94*, 3851-3866.

Forman, S.L., Lubinski, D.J., Miller, G.H., Snyder, J., Matishov, G.G., Korsun, S., & Myslivets, V. (1995). Postglacial emergence and distribution of Late Weichselian ice-sheet loads in the northern Barents and Kara Seas, Russia. *Geology*, *23*, 113–116

Gabrielsen, R.H., Faerseth, R.B., Jensen, L.N., Kalheim, J.E. & Riis, F. (1990). *Structural elements of the Norwegian continental shelf. Pt. 1. The Barents Sea region*. Norwegian Petroleum Directorate Bulletin, *6*, 33pp.

Gaina, C., Gernigon, L. & Ball, P. (2009). Palaeocene–Recent plate boundaries in the NE Atlantic and the formation of the Jan Mayen microcontinent. *Journal of the Geological Society*, *166*, 601-616.

Gjelberg, H.K. (2010). *Facies Analysis and Sandbody Geometry of the Paleogene Battfjellet Formation, Central Western Nordenskiöld Land, Spitsbergen*, MSc thesis, University of Bergen, Norway, 174pp.

Golovneva, L. (2010). Variability in epidermal characters of Ginkgo tzagajanica Samylina (Ginkgoales) from the Paleocene of the Tsagayan Formation (Amur region) and the taxonomy of Tertiary species of Ginkgo. *Paleontological Journal*, *44*, 584-594.

Greenwood, D.R., Basinger, J.F. & Smith, R.Y. (2010). How wet was the Arctic Eocene rain forest? Estimates of precipitation from Paleogene Arctic macrofloras. *Geology*, *38*, 15-18.

Grundvåg, S.-A., Johannessen, E.P., Helland-Hansen, W. & Plink-Björklund, P. (2014a). Depositional architecture and evolution of progradationally stacked lobe complexes in the Eocene Central Basin of Spitsbergen. *Sedimentology*, *61*, 535-569.

Grundvåg, S.-A., Helland-Hansen, W., Johannessen, E.P., Olsen, A.H. & Stene, S.A.K. (2014b). The depositional architecture and facies variability of shelf deltas in the Eocene Battfjellet Formation, Nathorst Land, Spitsbergen. *Sedimentology*, *61*, 2172-2204.

Hack, J.T. (1957). *Studies of longitudinal stream profiles in Virginia and Maryland*. U.S. Geological Survey Professional Paper, 294-B.

Hadler-Jacobsen, F., Johannessen, E., Ashton, N., Henriksen, S., Johnson, S. & Kristensen, J. (2005). Submarine fan morphology and lithology distribution: a predictable function of sediment delivery, gross shelf-to-basin relief, slope gradient and basin topography. In: *Geological Society, London, Petroleum Geology Conference Series*, *6*, pp. 1121-1145.

Haq, B.U. (2014). Cretaceous eustasy revisited. *Global and Planetary Change*, *113*, 44-58.

Harding, I.C., Charles, A.J., Marshall, J.E.A., Pälike, H., Roberts, A.P., Wilson, P.A., Jarvis, E., Thorne, R., Morris, E., Moremon, R., Pearce, R.B. & Akbari, S. (2011). Sea-level and salinity fluctuations during the Paleocene–Eocene thermal maximum in Arctic Spitsbergen. *Earth and Planetary Science Letters*, *303*, 97-107.

Helland-Hansen, W. (1985). *Sedimentology of the Battfjellet Formation (Palaeogene) in Nordenskiold Land, Spitsbergen,* Cand.scient. thesis, University of Bergen, Norway, 322p.

Helland-Hansen, W. (1990). Sedimentation in Paleogene foreland basin, Spitsbergen. *American Association of Petroleum Geologists Bulletin*, *74*, 260-272.

Helland-Hansen, W. (1992). Geometry and facies of Tertiary clinothems, Spitsbergen. *Sedimentology*, *39*, 1013-1029.

Helland-Hansen, W. (2010). Facies and stacking patterns of shelf-deltas within the Palaeogene Battfjellet Formation, Nordenskiöld Land, Svalbard: implications for subsurface reservoir prediction. *Sedimentology*, *57*, 190-208.

Helland-Hansen, W., Grundvåg, S.A. & Aadland, T. (2017). Assessment of duration of basin filling without chronostratigraphic data: a case study from the Cenozoic foreland basin of Spitsbergen. *International Meeting of Sedimentology* 2017, Toulouse (abstract).

Hodgson, D.M., Flint, S.S., Hodgetts, D., Drinkwater, N.J., Johannessen, E.P. & Luthi, S.M. (2006). Stratigraphic evolution of fine-grained submarine fan systems, Tanqua depocenter, Karoo Basin, South Africa. *Journal of Sedimentary Research*, *76*, 20-40.

Hoy, R.G. & Ridgway, K.D. (2003). Sedimentology and sequence stratigraphy of fan-delta and river-delta deposystems, Pennsylvanian Minturn Formation, Colorado. *American Association of Petroleum Geologists Bulletin, 87*, 1169-1191.

Ingersoll, R.V. (1988). Tectonics of sedimentary basins. *Geological Society of America Bulletin*, *100*, 1704-1719.

Jochmann, M. M., Augland, L. E., Lenz, O., Bieg, G., Haugen, T., Grundvåg, S. A., Jelby, M.E., Midtkandal, I., Dolezych, M. & Hjálmarsdóttir, H. R. (2019). Sylfjellet: a new outcrop of the Paleogene Van Mijenfjorden Group in Svalbard. *Arktos*, 1-22.

Johannessen, E.P. & Steel, R.J. (2005). Shelf-margin clinoforms and prediction of deepwater sands. *Basin Research*, *17*, 521-U34.

Jørgensen, K.W. (2015). *Sedimentology of inter-channel deposits of the Aspelintoppen Formation, Brogniartfjella, Svalbard.* MSc thesis, University of Bergen, Norway, 72pp.

Kellogg, H.E. (1975). Tertiary stratigraphy and tectonism in Svalbard and continental drift. *American Association of Petroleum Geologists Bulletin*, *59*, 465-485.

Knies, J., Matthiessen, J., Vogt, C., Laberg, J.S., Hjelstuen, B.O., Smelror, M., Larsen, E., Andreassen, K., Eidvin, T. & Vorren, T.O. (2009). The Plio-Pleistocene glaciation of the Barents Sea–Svalbard region: a new model based on revised chronostratigraphy. *Quaternary Science Reviews*, *28*, 812-829.

Kongsgården, A.G. (2016). *Sedimentology of channel-deposits of the Aspelintoppen Formation, Brogniartfjella, Svalbard*. MSc thesis, University of Bergen, Norway, 98pp.

Kristensen, T.B., Rotevatn, A., Marvik, M., Henstra, G.A., Gawthorpe, R.L. & Ravnås, R. (2018). Structural evolution of sheared margin basins: the role of strain partitioning. Sørvestsnaget Basin, Norwegian Barents Sea. *Basin Research*, *30*, 279-301.

Kvaček, Z. (1994). Connecting links between the Arctic Palaeogene and European Tertiary floras. In M.C. Boulter & H.C. Fisher (Eds.), *Cenozoic plants and climates of the Arctic*, *NATO ASI Series, I 27*, 251-266.

Landvik, J.Y., Bondevik, S., Elverhøi, A., Fjeldskaar, W., Mangerud, J., Salvigsen, O., Siegert, M.J., Svendsen, J.-I. & Vorren, T.O. (1998). The last glacial maximum of Svalbard and the Barents Sea area: ice sheet extent and configuration. *Quaternary Science Reviews*, *17*, 43-75.

Lasabuda, A.P.E., Laberg, J.S., Knutsen, S.-M. & Safronova, P. (2018). Cenozoic tectonostratigraphy and pre-glacial erosion: A mass-balance study of the northwestern Barents Sea margin. *Journal of Geodynamics, 119*, 149-166.

Lundin, E. & Doré, A. (2002). Mid-Cenozoic post-breakup deformation in the 'passive'margins bordering the Norwegian–Greenland Sea. *Marine and Petroleum Geology*, *19*, 79-93.

Løseth, T.M., Steel, R.J., Crabaugh, J.P. & Schellpeper, M. (2006). Interplay between shoreline migration paths, architecture and pinchout distance for siliciclastic shoreline tongues: evidence from the rock record. *Sedimentology, 53*, 735–767.

Macdonald, H.A., Peakall, J., Wignall, P.B. & Best, J. (2011). Sedimentation in deep-sea lobe-elements: implications for the origin of thickening-upward sequences. *Journal of Geological Society*, *168*, 319-332.

Major, H. & Nagy, J. (1972). Geology of the Adventdalen map area: with a geological map, Svalbard C9G 1: 100 000. *Norsk Polarinstitutt skrifter, 138*, 1-58.

Mansurbeg, H., Morad, S., Plink-Bjorklund, P., El-Ghali, M.A.K., Caja, M.A. & Marfil, R. (2012). Diagenetic alterations related to falling stage and lowstand systems tracts of shelf, slope and basin floor sandstones (Eocene Central Basin, Spitsbergen). *International Association of Sedimentologists Special Publication*, *45*, 353-378.

Manum, S.B. & Throndsen, T. (1978). Rank of coal and dispersed organic matter and its geological bearing in the Spitsbergen Tertiary. *Norsk Polarinstitutt Årbok*, *1977*, 159-177.

Manum, S.B. & Throndsen, T. (1986). Age of Tertiary formations on Spitsbergen. *Polar Research*, *4*, 103-131.

Marshall, C., Uguna, J., Large, D.J., Meredith, W., Jochmann, M., Friis, B., Vane, C., Spiro, B.F., Snape, C.E. & Orheim, A. (2015). Geochemistry and petrology of palaeocene coals from Spitzbergen—Part 2: Maturity variations and implications for local and regional burial models. *International Journal of Coal Geology*, *143*, 1-10.

Mellere, D., Plink-Bjorklund, P. & Steel, R. (2002). Anatomy of shelf deltas at the edge of a prograding Eocene shelf margin, Spitsbergen. *Sedimentology*, *49,* 1181-1206.

Mellere, D., Breda, A., & Steel, R.J. (2003). Fluvially incised shelf-edge deltas and linkage to upper-slope channels (Central Tertiary Basin, Spitsbergen). In N.C.R. H.H. Roberts, R.H. Fillon & J.B. Anderson (Eds.), *Shelf-Margin Deltas and Linked downslope Petroleum Systems,* (pp. 231-266, CD-ROM). Gulf Coast Section SEPM 23rd Annual Research Conference Proceedings.

Meng, Q.-R., Wang, E. & Hu, J.-M. (2005). Mesozoic sedimentary evolution of the northwest Sichuan basin: Implication for continued clockwise rotation of the South China block. *Geological Society of America Bulletin*, *117,* 396-410.

Miller, K.G., Kominz, M.A., Browning, J.V., Wright, J.D., Mountain, G.S., Katz, M.E., Sugarman, P.J., Cramer, B.S., Christie-Blick, N. & Pekar, S.F. (2005). The Phanerozoic record of global sea-level change. *Science*, *310,* 1293-1298.

Mutti, E., Davoli, G., Tinterri, R. & Zavala, C. (1996). The importance of ancient fluvio-deltaic systems dominated by catastrophic flooding in tectonically active basins. *Memorie di Scienze Geologiche*, *48*, 233-291.

Mutti, E., Tinterri, R., Benevelli, G., Di Biase, D., & Cavanna, G. (2003). Deltaic, mixed and turbidite sedimentation of ancient foreland basins. *Marine and Petroleum Geology, 20*, 733-755.

Nathorst, A.G. (1910). Beiträge zur Geologie der Bären-Insel, Spitzbergens und des König-Karl-Landes. *Bulletin of the Geological Institution of the University of Uppsala, 10*, 261-415.

Naurstad, O.A. (2014). *Sedimentology of the Aspelintoppen Formation (Eocene-Oligocene), Brogniartfjella, Svalbard*, MSc thesis, University of Bergen, Norway, 124 pp.

Nilsen, T.H. & Sylvester, A.G. (1999). Strike-slip basins: Part 1. *The Leading Edge*, *18*, 1146-1152.

Nysæther, E. (1966). *Petrografisk undersøkelse av sedimentære bergarter fra tidsperioden kritt-tertiær i Nathorst Land, Vest Spitsbergen.* Cand. Real. Thesis, University of Bergen, Norway, 168 pp.

Olsen, A. (2008). *Sedimentology and paleogeography of the Battfjellet Fm. Southern Van Mijenfjorden, Svalbard.* MSc thesis, University of Bergen, Bergen, Norway, 91 pp.

Osen, T.G. (2012). *Facies, Sandbody Geometry and Palaeogeography of the Battfjellet Formation, Urdkolldalen area, Nordenskiold Land, Svalbard*. MSc thesis, University of Bergen, Bergen, Norway. 90pp

Petersen, T.G., Thomsen, T., Olaussen, S. & Stemmerik, L. (2016). Provenance shifts in an evolving Eurekan foreland basin: the Tertiary Central Basin, Spitsbergen. *Journal of the Geological Society*, *173*, 634-648.

Petter, A.L. & Steel, R.J. (2006). Hyperpycnal flow variability and slope organization on an Eocene shelf margin, Central Basin, Spitsbergen. *American Association of Petroleum Geologists Bulletin*, *90*, 1451-1472.

Piepjohn, K., von Gosen, W. & Tessensohn, F. (2016). The Eurekan deformation in the Arctic: an outline. *Journal of the Geological Society*, *173*, 1007-1024.

Plink-Bjorklund, P., Mellere, D. & Steel, R.J. (2001). Turbidite variability and architecture of sand-prone, deep-water slopes: Eocene clinoforms in the Central Basin, Spitsbergen. *Journal of Sedimentary Research*, *71*, 895-912.

Plink-Björklund, P. & Steel, R. J. (2002). Sea-level fall below the shelf edge, without basin-floor fans. *Geology*, *30*(2), 115-118.

Plink-Björklund, P. (2005). Stacked fluvial and tide-dominated estuarine deposits in high-frequency (fourth-order) sequences of the Eocene Central Basin, Spitsbergen. *Sedimentology*, *52*, 391-428.

Plink-Björklund, P. & Steel, R. (2005). Deltas on falling-stage and lowstand shelf margins, the Eocene Central Basin of Spitsbergen: importance of sediment supply. *SEPM Special Publication*, *83*, 179-206.

Plink-Björklund, P. & Steel, R. (2006). Incised valleys on an Eocene coastal plain and shelf, Spitsbergen—part of a linked shelf–slope system. *SEPM Special Publication*, *85*, 281-307.

Ponten, A. & Plink-Bjorklund, P. (2009). Process Regime Changes Across a Regressive to Transgressive Turnaround in a Shelf-Slope Basin, Eocene Central Basin of Spitsbergen. *Journal of Sedimentary Research*, *79*, 2-23.

Posamentier, H. & Allen, G. (1993). Siliciclastic sequence stratigraphic patterns in foreland, ramp-type basins. *Geology*, *21*, 455-458.

Potter, P. & Pettijohn, F. (1963). *Paleocurrents and basin analysis*. Academic Press Inc. New York, 296 pp.

Prélat, A., Hodgson, D. & Flint, S. (2009). Evolution, architecture and hierarchy of distributary deep-water deposits: a high-resolution outcrop investigation from the Permian Karoo Basin, South Africa. *Sedimentology*, *56*, 2132-2154.

Rasmussen, E., Skott, P.H. & Larsen, K.-B. (1995). Hydrocarbon potential of the Bjørnøya West Province, western Barents Sea Margin. *Norwegian Petroleum Society Special Publication*, 4, pp. 277-286.

Ryseth, A., Augustson, J.H., Charnock, M., Haugerud, O., Knutsen, S.-M., Midbøe, P.S., Opsal, J.G. & Sundsbø, G. (2003). Cenozoic stratigraphy and evolution of the Sørvestsnaget Basin, southwestern Barents Sea. *Norwegian Journal of Geology 83*, 107-130.

Safronova, P.A., Henriksen, S., Andreassen, K., Laberg, J.S. & Vorren, T.O. (2014). Evolution of shelf-margin clinoforms and deep-water fans during the middle Eocene in the Sorvestsnaget Basin, southwest Barents Sea. *American Association of Petroleum Geologists Bulletin*, *98*, 515-544.

Sanderson, D.J. & Marchini, W. (1984). Transpression. *Journal of Structural Geology*, *6*, 449-458.

1049 Schlegel, A., Lisker, F., Dörr, N., Jochmann, M., Schubert, K. & Spiegel, C. (2013). Petrography and geochemistry of
1050 siliciclastic rocks from the Central Tertiary Basin of Svalbard - implications for provenance, tectonic
1051 setting and climate. *Zeitschrift der Deutschen Gesellschaft für Geowissenschaften*, *164*, 173-186.
1052

1053 Skarpeid, S.S. (2010). *Facies Architecture and Paleogeography of the Battfjellet Formation, Rypefjellet, Spitsbergen*,
1054 MSc thesis, University of Bergen, Norway, 113 pp.
1055

1056 Smelror, M., Petrov, O., Larssen, G.B. & Werner, S. (2009). *Atlas: Geological history of the Barents Sea*. Norges
1057 Geologiske Undersøkelse, 135pp.
1058

1059 Steel, R.J. (1977). Observations on some Cretaceous and Tertiary sandstone bodies in Nordenskiöld Land, Svalbard,
1060 *Norsk Polarinstitutt Årbok*, *1976,* 43-68.
1061
1062 Steel, R., Dalland, A., Kalgraff, K. & Larsen, V. (1981). The Central Tertiary Basin of Spitsbergen: sedimentary
1063 development of a Sheared-Margin Basin. In J.W. Kerr & A.J. Ferguson (Eds.), *Geology of the North Atlantic*
1064 *Borderland* (Vol. *7*, pp. 647-664). Canadian Society of Petroleum Geologists Memoir.
1065
1066 Steel, R., Gjelberg, J., Helland-Hansen, W., Kleinspehn, K., Nøttvedt, A. & Rye-Larsen, M. (1985). The Tertiary strike-
1067 slip basins and orogenic belt of Spitsbergen. *SEPM Special Publication, 37*, 339-359.
1068
1069 Steel, R.J., Crabaugh, J.P., Schellpeper, M., Mellere, D., Plink-Bjorklund, P., Deibert, J. & Løseth, T.M. (2000). Deltas
1070 versus rivers on the shelf edge: their relative contributions to the growth of shelf margins and basin-floor
1071 fans (Barremian and Eocene, Spitsbergen). In P. Weimer, R.M. Slatt, J. Coleman, N.C. Rosen, H. Nelson,
1072 A.H. Bouma, M.J. Styzen & D.T. Lawrence (Eds.), *Deep-Water Reservoirs of the World* (pp. 981-1009). Gulf
1073 Coast Section SEPM 20th Annual Research Conference Proceedings.
1074
1075 Steel, R.J. & Olsen, T. (2002). Clinoforms, Clinoform Trajectories and Deepwater Sands. In J.M. Armentrout & N.C.
1076 Rosen (Eds.), *Sequence Stratigraphic Models for Exploration and Production: Evolving Methodology,*
1077 *Emerging Models and Application Histories* (pp. 367-381, CD-ROM). Gulf Coast Section SEPM 22th Annual
1078 Research Conference Proceedings.
1079

1080 Stene, S.A.K. (2008). *Facies and architecture of the Battfjellet Formation, northern Nathorst Land, Spitsbergen.* MSc
1081 thesis, University of Bergen, Norway, 103pp.

1082 Tegner, C., Storey, M., Holm, P.M., Thorarinsson, S., Zhao, X., Lo, C.-H. & Knudsen, M.F. (2011). Magmatism and
1083 Eurekan deformation in the High Arctic Large Igneous Province: 40 Ar–39 Ar age of Kap Washington
1084 Group volcanics, North Greenland. *Earth and Planetary Science Letter*, *303*, 203-214.
1085

1086 Uhl, D., Traiser, C., Griesser, U. & Denk, T. (2007). Fossil leaves as palaeoclimate proxies in the Palaeogene of
1087 Spitsbergen (Svalbard). *Acta Palaeobotanica Krakow*, *47*, 89.
1088
1089 Uroza, C.A. & Steel, R.J. (2008). A highstand shelf-margin delta system from the Eocene of West Spitsbergen,
1090 Norway. *Sedimentary Geology*, *203*, 229-245.
1091

1092 Van Wagoner, J.C., Mitchum, R.M., Campion, K.M. & Rahmanian, V.D. (1990). Siliciclastic sequence stratigraphy in
1093 well logs, cores, and outcrops: Concepts for high resolution correlation of time and facies. *American*
1094 *Association of Petroleum Geologists, Methods in Exploration Series*, *7*, 55pp.
1095

Willis, A. (2000). Tectonic control of nested sequence architecture in the Sego Sandstone, Neslen Formation and upper Castlegate Sandstone (Upper Cretaceous), Sevier foreland basin, Utah, USA. *Sedimentary Geology*, *136*, 277-317.

Zhang, G.-B. & Bott, M.H. (2000). Modelling the evolution of asymmetrical basins bounded by high-angle reverse faults with application to foreland basins. *Tectonophysics*, *322*, 203-218.

FIGURE CAPTIONS:

Figure 1. Location of study area. Insert map shows location of logged sections that are compiled from our own data and publications, and MSc theses (for references, see paragraph "Data"). Geological map modified from Dallmann & Elvevold (2015) and Jochmann et al. (2019). HFZ: Hornsund Fault Zone; SFZ: Senja Fracture Zone; SB: Sørvestsnaget Basin; SH: Stappen High; VVP: Vestbakken Volcanic Province; WSFTB: West Spitsbergen Fold-and-thrust Belt; CB: Central Basin; L: Lars Hiertafjellet; S: Sven Nilssonfjellet; V. Vengefjellet; P: Pallfjellet; B: Brogniartfjella; D: Drevfjellet; H: Hyrnestabben.

Figure 2. Stratigraphy of the Central Basin Paleogene succession. Modified from Grundvåg et al., 2014a.

Figure 3. The cored section of the Sysselmannbreen Well (cf. Figure1 for location) showing lithology, gamma-ray and breakdown of environmental elements of the Frysjaodden, Battfjellet and Aspelintoppen Formations and their underlying Basilika and Grumantbyen formations. Modified from Grundvåg et al., 2014a.

Figure 4 (cf. Figure 1 for map outline and legend, data in maps A-F compiled from MSc theses and our own data and publications, for references, see paragraph "Data")**.** A) Preserved thickness of the of the combined Hollendardalen Formation, Gilsonryggen Member and Battfjellet Formation; B) Composite isopach thickness of the combined Hollendardalen Formation, Gilsonryggen Member and Battfjellet Formation (inferred thicknesses in areas where present day erosion extends into the Battfjellet and underlying formations) ; C) Number of parasequences (>5m) in the Battfjellet Formation at logged localities; D) Wave-ripple crest orientations compiled from logged sections and summarized for four sub-areas; E) Dip azimuths of current-ripple cross-lamination at shelf-edge to upper slope positions (rose diagram) and apparent clinoform dip directions/slope angles. Note that clinoforms are concentrated in the western part of the study area; F) Location of logged sections with turbidite lobe complexes (note that these are concentrated in two zones) and dip azimuths of current-ripple cross-lamination (for Zone 1 (left) and Zone 2 (right), respectively).

Figure 5. Overview photos of environmental elements within the GBA-unit: A) The mountain Storvola in Van Keulenfjorden viewed towards northwest showing coastal plain (CP), shelf-delta (SD), slope (S), basin floor (BF) and deepwater shale (DS) elements (width of mountain about 6km) ; B) stacked coarsening-upwards (CU) shelf-delta parasequences with intervening flooding surfaces (FS, stipled lines) at Drevfjellet; C) transition from slope to shelf-edge deltas and shelf-deltas at the south side of

Sven Nilssonfjellet; D) superimposed slope, shelf-edge, shelf-delta and coastal plain sediments at Brogniartfjella, Van Keulenfjorden. Note sloping shelf-edge delta wedge; E) Storvola in Van Keulenfjorden viewed towards southeast showing coastal plain (CP), shelf-delta (SD), slope (S), basin floor (BF) and deepwater shale(DS) elements. For location of photos see Figure 1.

Figure 6. Logs through the different environmental elements in the GBA-unit showing grain-sizes, sedimentary structures, trace fossils and environmental interpretations (locations of logs (see Figure1): A Vengefjellet, B south side of Sven Nilssonfjellet, C western part of Brogniartfjella; D western Sven Nilssonfjellet, E Pallfjellet, F western Sven Nilssonfjellet , G Sysselmannbreen well, H Sysselmannbreen well and I Hyrnestabben).

Figure 7. Facies types from the different environmental elements in the GBA-unit (for locations of localities, see Figure 1):

A), B) and C): fine-grained coastal plain succession with coal bed (cores from the Sysselmannbreen well) (A), overbank sandstone sheets (from Brogniartfjella) (B), and channel sandstone body (stippled base) incising its associated and underlying overbank sheet (from Brogniartfjella) (C).

D), E) and F): shelf-delta successions showing a typical coarsening-upwards parasequence (from (Vengefjellet) (D), hummocky-cross-stratification (from Lars Hiertafjellet) (E) and ball-and-pillow structures which are common features within these parasequences (from Brogniartfjella) (F).

G): shelf-edge element showing stacked beds of soft-sediment deformed sandstones overlain by a sharp-based sandstone unit (from Brogniartfjella).

H) and I): slope lobe element with heterolithic sandstones organized into a crude upwards coarsening unit (from Storvola) (H), and thick-bedded and amalgamated erosionally based turbidite channel in a middle slope setting (from Pallfjellet) (I).

J): basin floor element with a small-scale thickening upward cycle consisting of a thick turbidite bed stacked on top of thinner turbidite beds. Such cycles internally characterize many of the turbidite lobes (from Hyrnestabben).

K): finely laminated basinal mudstones with laminations of siltstone (light coloured streaks), and siderite bands (rusty colour) (from Sysselmannbreen well).

Figure 8. Proposed paleogeographic maps for the GBA-unit at early stage of progradation when shorelines reaches local shelf-edges with accumulation of sandy slope wedges and basin-floor fans (A), when progradation has reached further into the shallower part of the basin (B) and finally, when the preserved part of the basin has been filled to sea-level with dominance of channel and inter-channel deposition (C). Paleocurrent measurements in fluvial channel deposits points to a slight southeasterly direction of outbuilding at the latter stage (cf .Helland-Hansen, 1990; Naurstad, 2014).

Figure 9. Basic architecture of an individual shelf-delta parasequence (for their stacking pattern, cf. Figure 10). Note that pinch-out distance normally will be longer than progradational distance for individual parasequences. This has the effect that parasequences when vertically stacked more commonly will terminate in shoreface/foreshore lithosomes than continental lithosomes. Also, since these units have their lithosomes defined according to vertically energy zonation in the water

column, facies-belt boundaries will be sub-horizontal. This is contrast to the clinothems where lithology drapes sloping depositional surfaces. FWWB=fair-weather wave-base, SWB=storm wave-base.

Figure 10. Southwest-to-northeast transect through the Gilsonryggen Member, and Battfjellet and Aspelintoppen formations showing environmental elements and time-space development of the succession. Stippled lines are hypothesized timelines. Deliberately we have showed an ascending trajectory of the system emphasizing its overall stratigraphic climb. Note also the shingled architecture of the Battfjellet Formation, the common termination of shelf parasequences in shallow-marine lithosomes (except the uppermost one that transitions into the Aspelintoppen Formation), the presence of shelf-edge, sandy slope and turbidite lobes of the basin floor elements limited to the western part of the basin and the gradual shallowing of the basin from west to east. Outline of insert map as for detailed map in Figure 1. Logs Pallfjellet and Sysselmannsbreen modified from Grundvåg et al., 2014a, log Rånekampen modified from Olsen, 2008, logs Urdkollbreen and Røystoppen modified from Osen, 2012).

Highlights:

- The studied succession accumulated in a foredeep zone of a foreland basin.
- The system drained from small catchments (500–1000 km^2) with sediments accumulating close (<100km) to the drainage divide.
- Progradation across the basin took place with an ascending shelf-edge trajectory.
- The succession is typified by a shingled architecture with limited lateral extent (3-6 km) of basinward-offset shallow marine lithosomes.
- Subsidence rates were high, probably preventing relative sea-level falls.

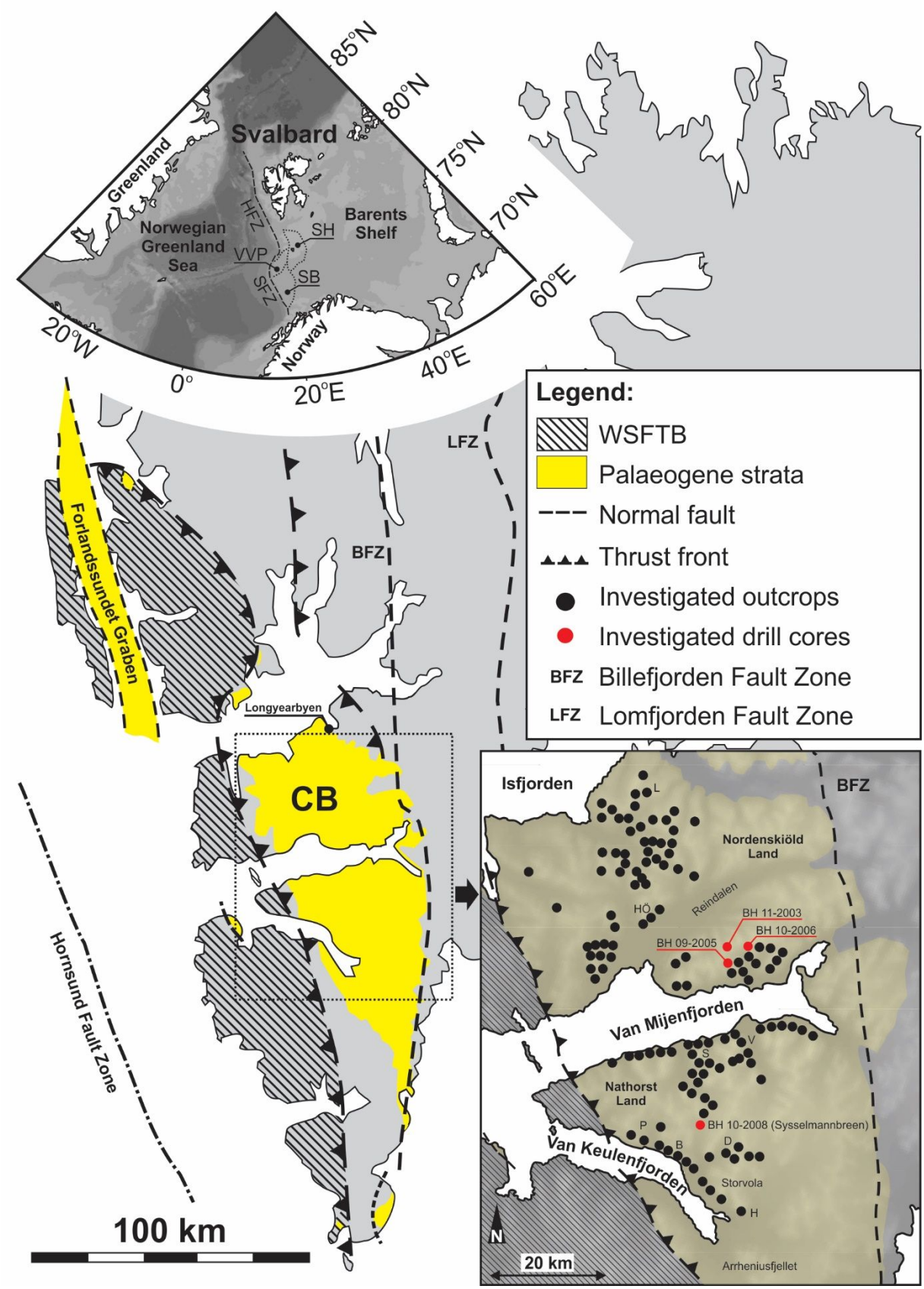
Svalbard
Greenland
Norwegian Greenland Sea
Barents Shelf
HFZ
SH
VVP
SB
SFZ
Norway
85°N
80°N
75°N
70°N
60°E
20°W
0°
20°E
40°E
Legend:
WSFTB
Palaeogene strata
Normal fault
Thrust front
Investigated outcrops
Investigated drill cores
BFZ Billefjorden Fault Zone
LFZ Lomfjorden Fault Zone
LFZ
BFZ
Forlandssundet Graben
Longyearbyen
CB
Hornsund Fault Zone
100 km
Isfjorden
BFZ
Nordenskiöld Land
Reindalen
HÖ
BH 11-2003
BH 10-2006
BH 09-2005
Van Mijenfjorden
Nathorst Land
BH 10-2008 (Sysselmannbreen)
Van Keulenfjorden
Storvola
Arrheniusfjellet
N
20 km

Figure 1

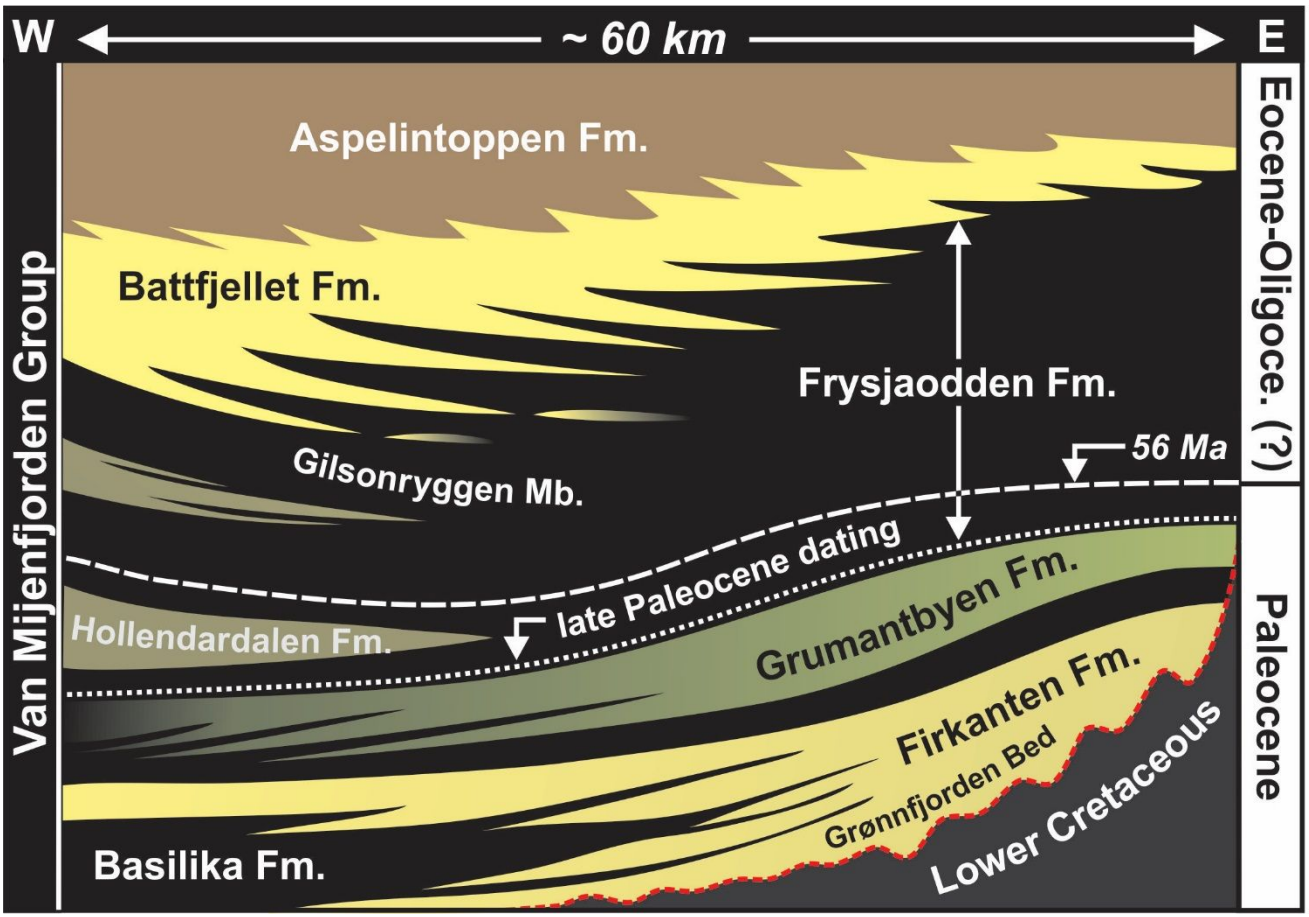
W
~ 60 km
E
Aspelintoppen Fm.
Battfjellet Fm.
Frysjaodden Fm.
56 Ma
Gilsonryggen Mb.
late Paleocene dating
Hollendardalen Fm.
Grumantbyen Fm.
Firkanten Fm.
Grønnfjorden Bed
Basilika Fm.
Lower Cretaceous
Van Mijenfjorden Group
Eocene-Oligoce. (?)
Paleocene

Figure 2

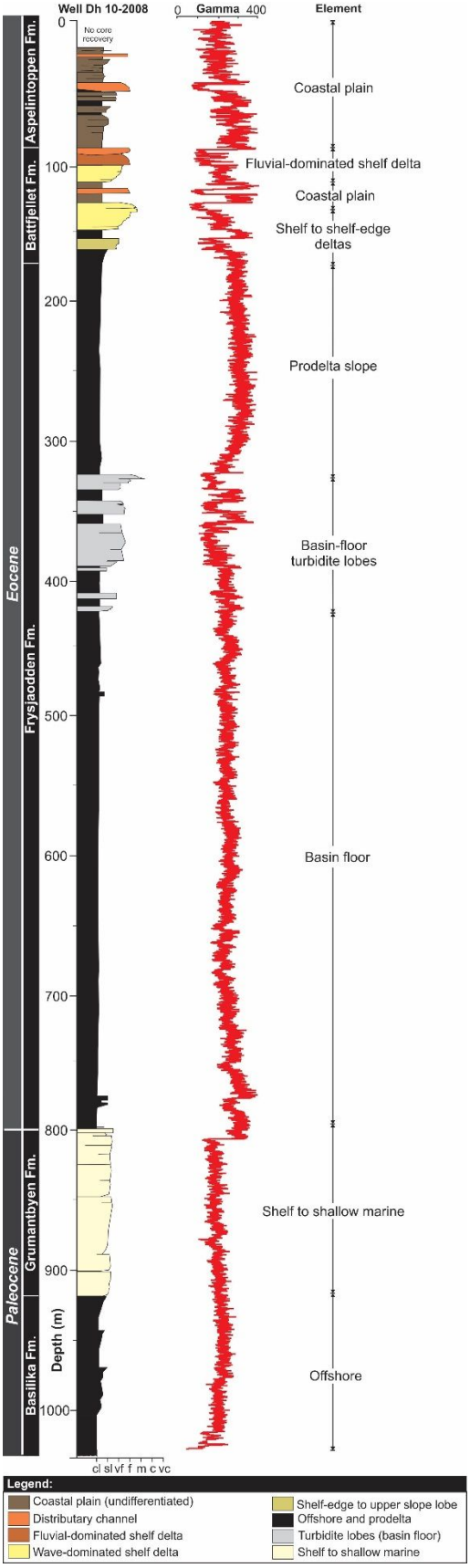
Well Dh 10-2008
0 Gamma 400
Element
No core recovery
Coastal plain
Fluvial-dominated shelf delta
Coastal plain
Shelf to shelf-edge deltas
Prodelta slope
Basin-floor turbidite lobes
Basin floor
Shelf to shallow marine
Offshore
Eocene
Paleocene
Aspelintoppen Fm.
Battfjellet Fm.
Frysjaodden Fm.
Grumantbyen Fm.
Basilika Fm.
Depth (m)
0
100
200
300
400
500
600
700
800
900
1000
cl sl vf f m c vc
Legend:
Coastal plain (undifferentiated)
Distributary channel
Fluvial-dominated shelf delta
Wave-dominated shelf delta
Shelf-edge to upper slope lobe
Offshore and prodelta
Turbidite lobes (basin floor)
Shelf to shallow marine

Figure 3

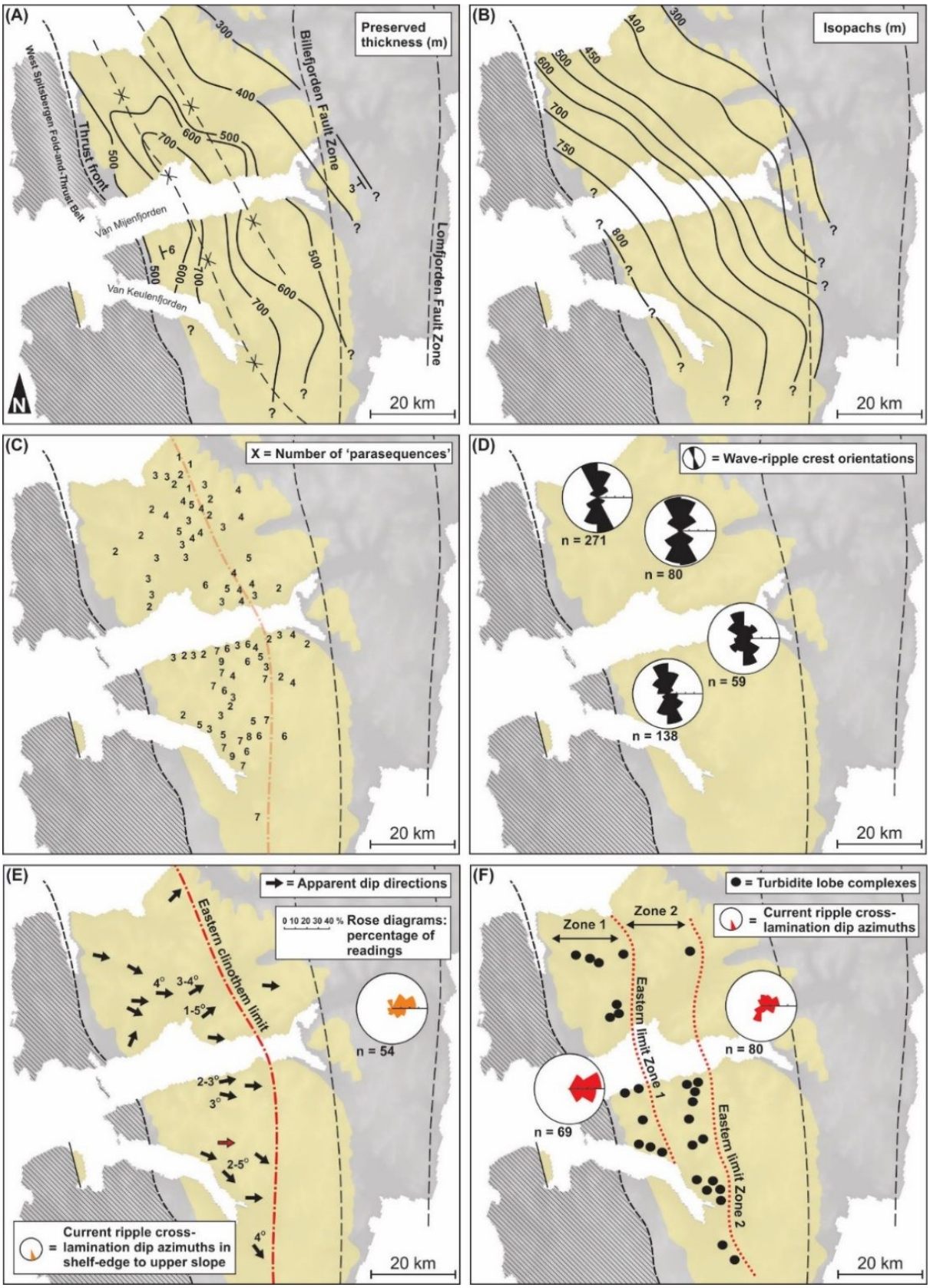
(A)
Preserved thickness (m)
West Spitsbergen Fold-and-Thrust Belt
Thrust front
Billefjorden Fault Zone
Lomfjorden Fault Zone
Van Mijenfjorden
Van Keulenfjorden
300
400
500
600
700
N
20 km
(B)
Isopachs (m)
300
400
450
500
600
700
750
800
20 km
(C)
X = Number of 'parasequences'
20 km
(D)
= Wave-ripple crest orientations
n = 271
n = 80
n = 59
n = 138
20 km
(E)
= Apparent dip directions
Eastern clinothem limit
0 10 20 30 40 % Rose diagrams: percentage of readings
n = 54
4°
3-4°
1-5°
2-3°
3°
2-5°
4°
Current ripple cross-lamination dip azimuths in shelf-edge to upper slope
20 km
(F)
= Turbidite lobe complexes
Zone 1
Zone 2
= Current ripple cross-lamination dip azimuths
Eastern limit Zone 1
Eastern limit Zone 2
n = 80
n = 69
20 km

Figure 4

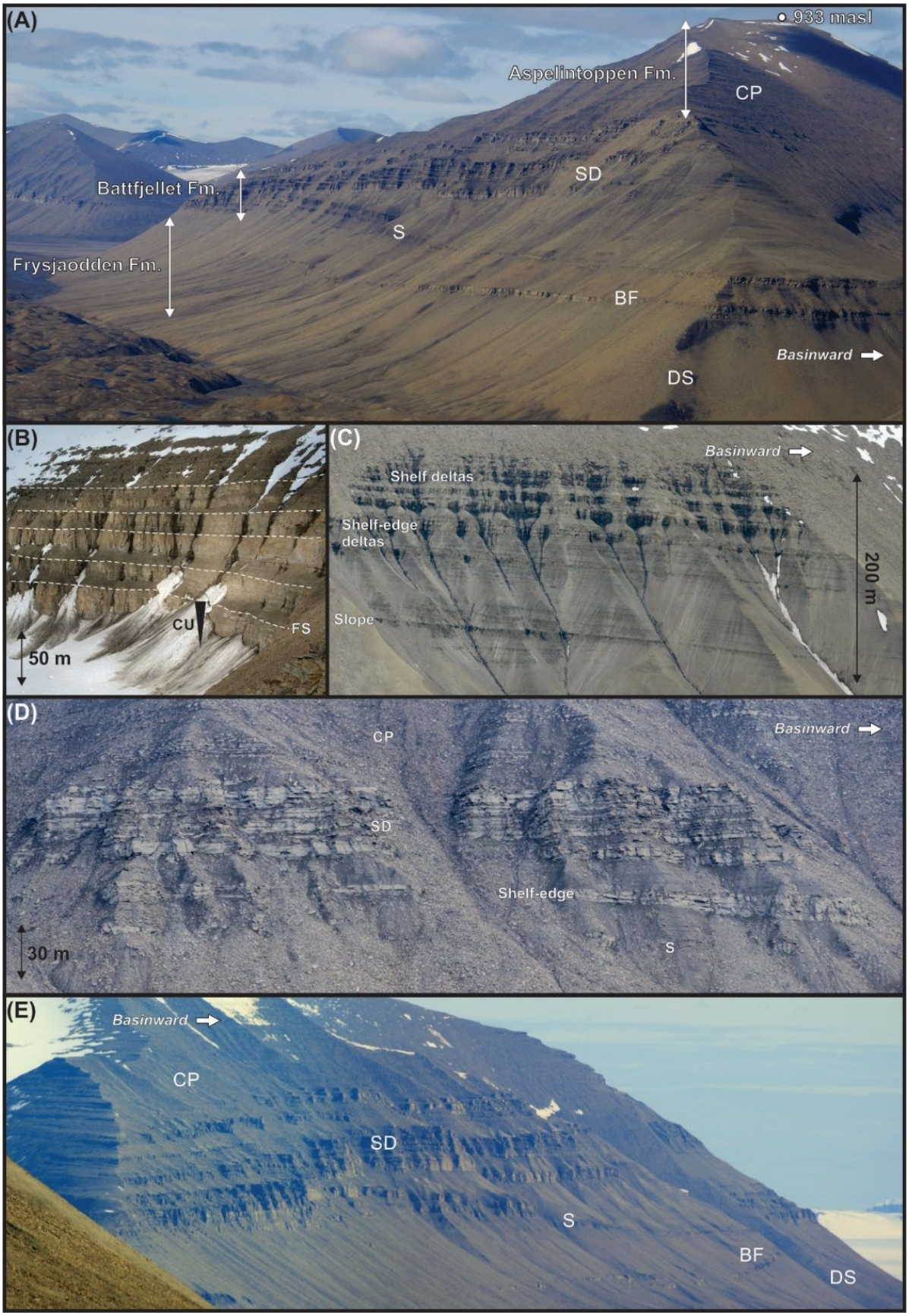
(A)
933 masl
Aspelintoppen Fm.
CP
SD
Battfjellet Fm.
S
Frysjaodden Fm.
BF
Basinward
DS
(B)
CU
FS
50 m
(C)
Basinward
Shelf deltas
Shelf-edge deltas
Slope
200 m
(D)
CP
Basinward
SD
Shelf-edge
30 m
S
(E)
Basinward
CP
SD
S
BF
DS

Figure 5

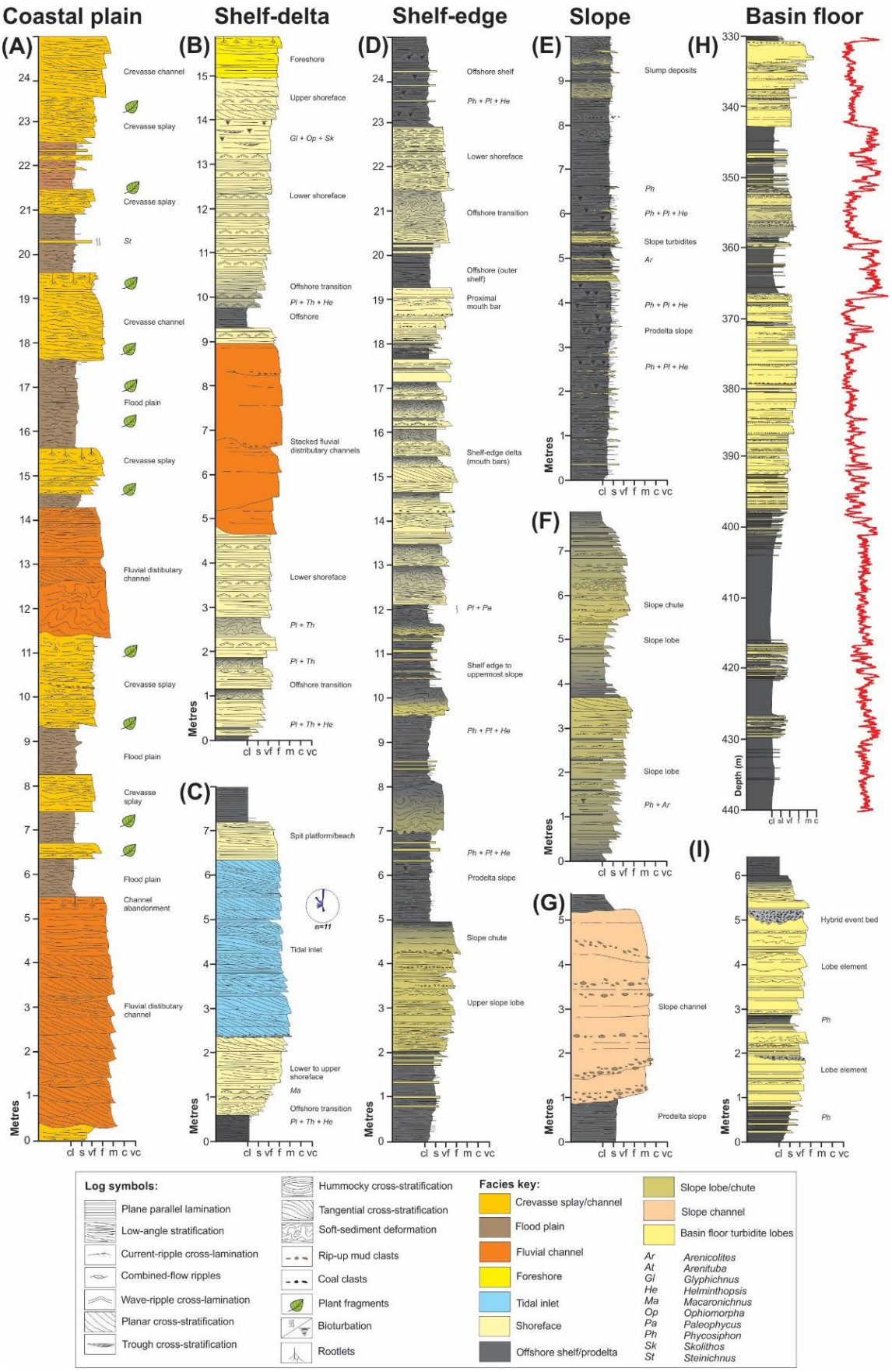
Coastal plain
Shelf-delta
Shelf-edge
Slope
Basin floor
(A)
(B)
(C)
(D)
(E)
(F)
(G)
(H)
(I)
Metres
Depth (m)
cl s vf f m c vc
Crevasse channel
Crevasse splay
St
Flood plain
Fluvial distibutary channel
Channel abandonment
Foreshore
Upper shoreface
Gl + Op + Sk
Lower shoreface
Offshore transition
Pl + Th + He
Offshore
Stacked fluvial distributary channels
Pl + Th
Spit platform/beach
n=11
Tidal inlet
Lower to upper shoreface
Ma
Offshore shelf
Ph + Pl + He
Proximal mouth bar
Shelf-edge delta (mouth bars)
Pl + Pa
Shelf edge to uppermost slope
Prodelta slope
Slope chute
Upper slope lobe
Slump deposits
Ph
Slope turbidites
Ar
Slope lobe
Ph + Ar
Slope channel
Hybrid event bed
Lobe element
Log symbols:
Plane parallel lamination
Low-angle stratification
Current-ripple cross-lamination
Combined-flow ripples
Wave-ripple cross-lamination
Planar cross-stratification
Trough cross-stratification
Hummocky cross-stratification
Tangential cross-stratification
Soft-sediment deformation
Rip-up mud clasts
Coal clasts
Plant fragments
Bioturbation
Rootlets
Facies key:
Crevasse splay/channel
Flood plain
Fluvial channel
Foreshore
Tidal inlet
Shoreface
Offshore shelf/prodelta
Slope lobe/chute
Slope channel
Basin floor turbidite lobes
Ar Arenicolites
At Arenituba
Gl Glyphichnus
He Helminthopsis
Ma Macaronichnus
Op Ophiomorpha
Pa Paleophycus
Ph Phycosiphon
Sk Skolithos
St Steinichnus

Figure 6

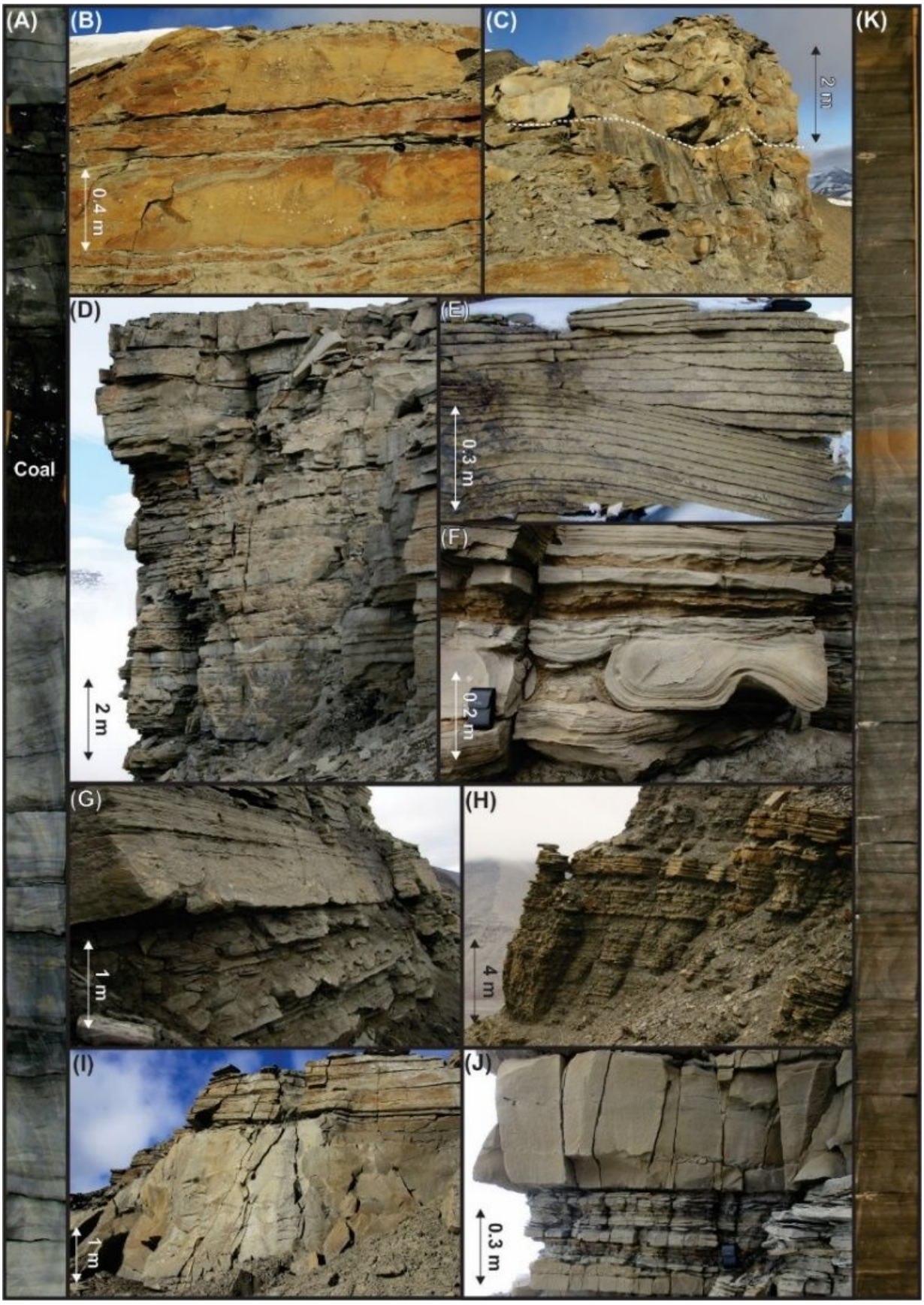

Figure 7

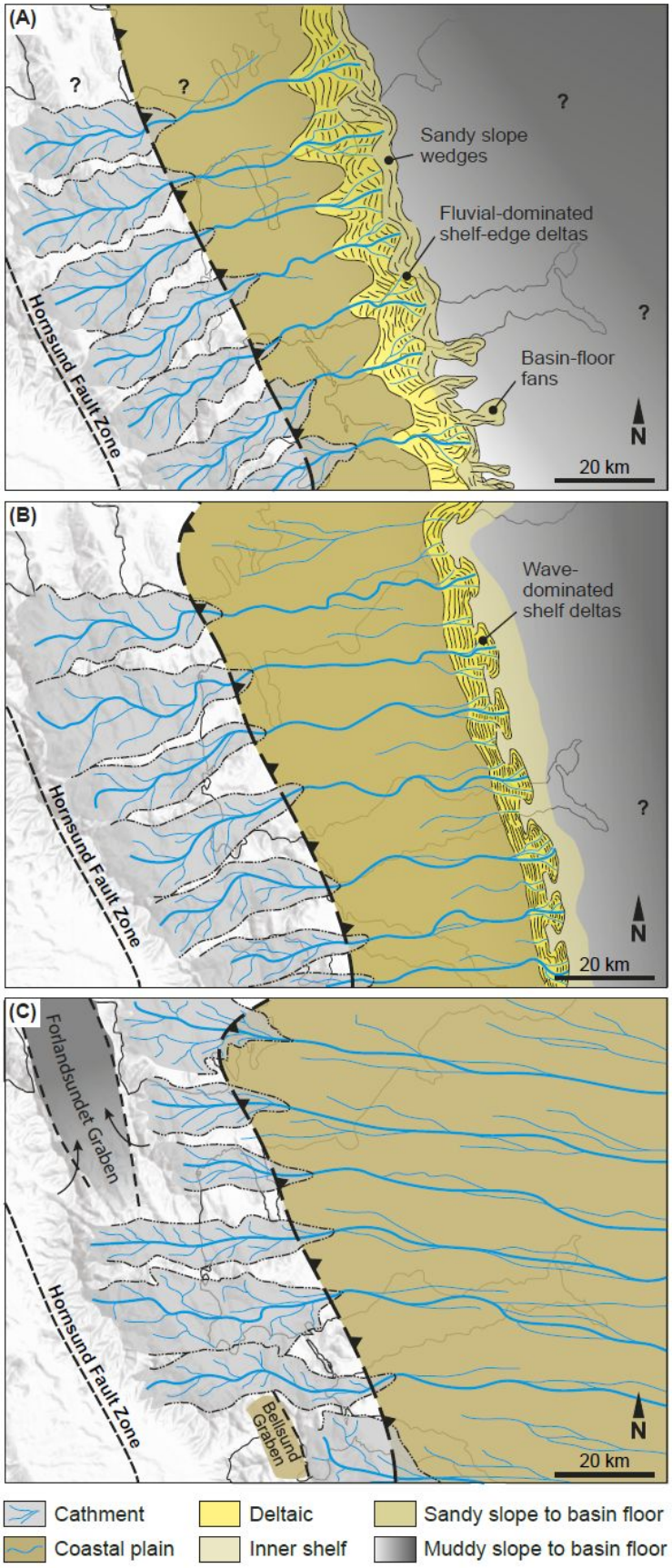
(A)
?
?
?
?
Sandy slope wedges
Fluvial-dominated shelf-edge deltas
Basin-floor fans
Hornsund Fault Zone
N
20 km
(B)
Wave-dominated shelf deltas
Hornsund Fault Zone
?
N
20 km
(C)
Forlandsundet Graben
Hornsund Fault Zone
Bellsund Graben
N
20 km
Cathment
Coastal plain
Deltaic
Inner shelf
Sandy slope to basin floor
Muddy slope to basin floor

Figure 8

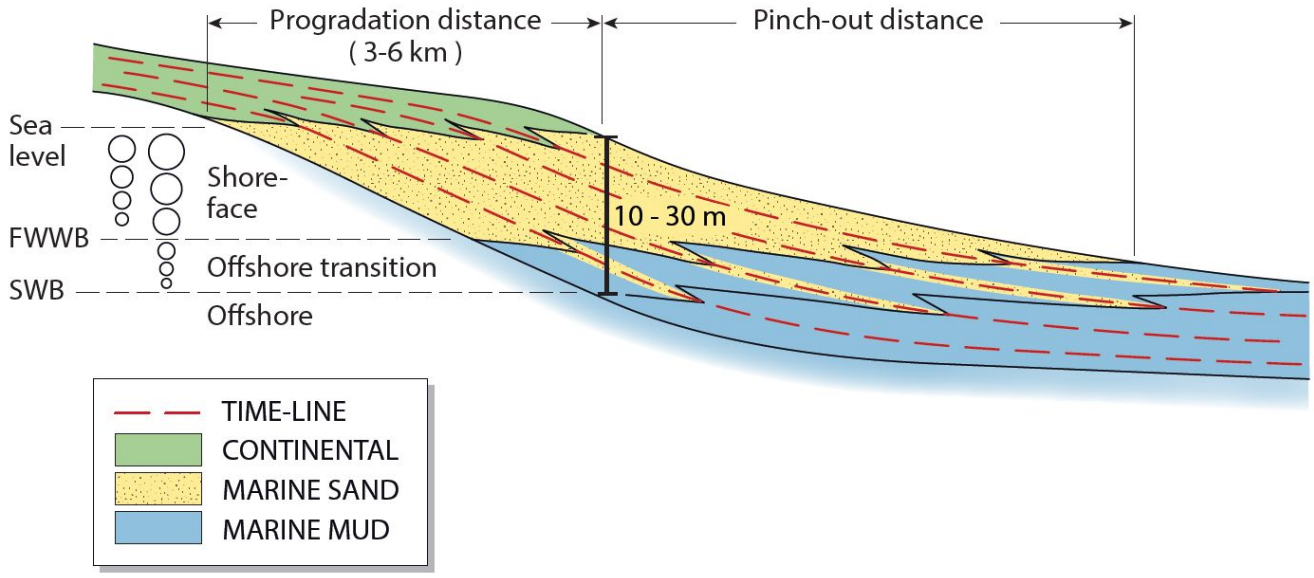
Progradation distance
(3-6 km)
Pinch-out distance
Sea
level
Shore-
face
FWWB
Offshore transition
SWB
Offshore
10 - 30 m
TIME-LINE
CONTINENTAL
MARINE SAND
MARINE MUD

Figure 9

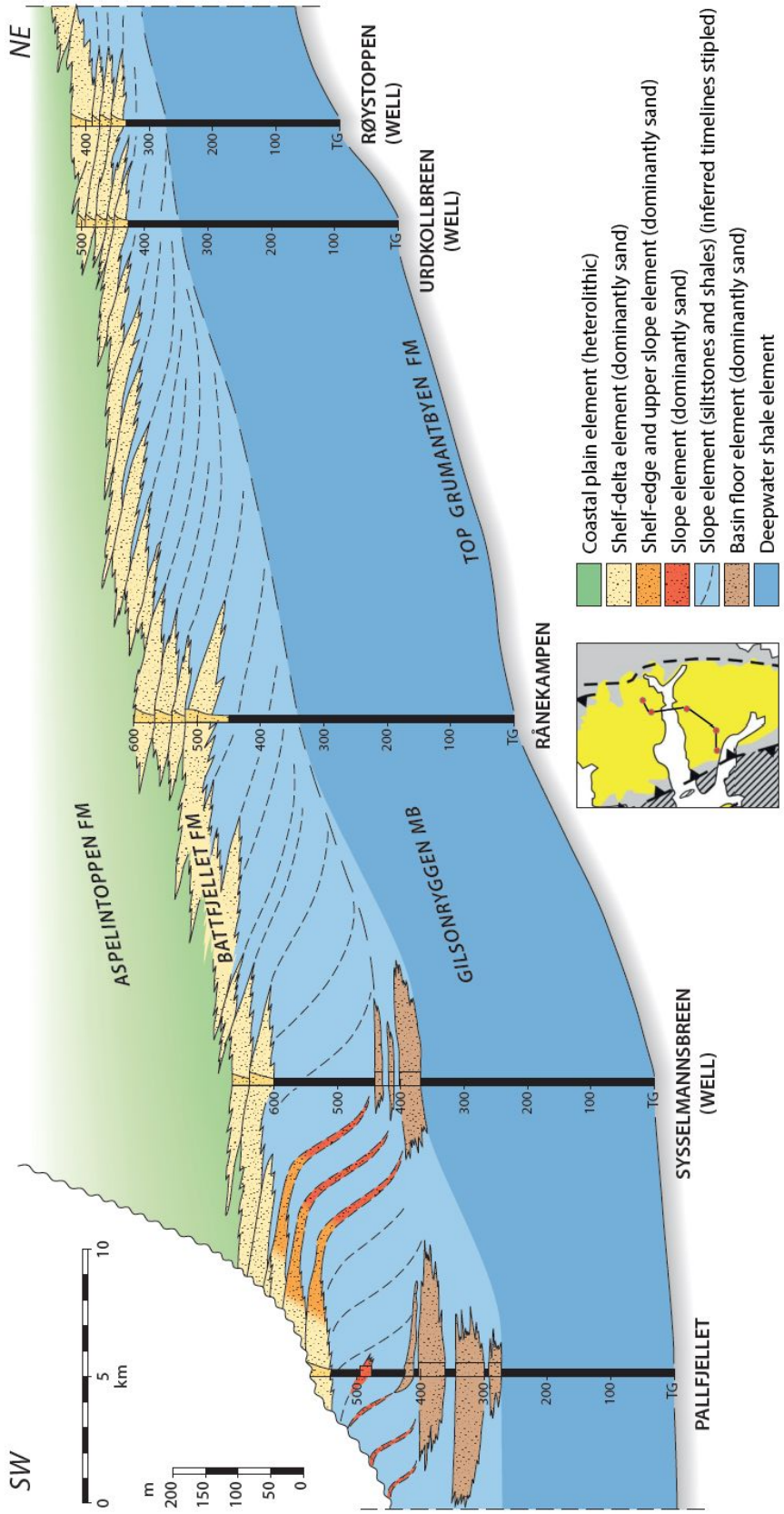
NE
SW
RØYSTOPPEN (WELL)
URDKOLLBREEN (WELL)
RÅNEKAMPEN
SYSSELMANNSBREEN (WELL)
PALLFJELLET
TOP GRUMANTBYEN FM
ASPELINTOPPEN FM
BATTFJELLET FM
GILSONRYGGEN MB
TG
0
5
10
km
m
200
150
100
50
0
Coastal plain element (heterolithic)
Shelf-delta element (dominantly sand)
Shelf-edge and upper slope element (dominantly sand)
Slope element (dominantly sand)
Slope element (siltstones and shales) (inferred timelines stipled)
Basin floor element (dominantly sand)
Deepwater shale element

Figure 10